

# CLASSICAL FOUNDATIONS OF MANY-PARTICLE QUANTUM CHAOS

BORIS GUTKIN, VLADIMIR OSIPOV

**ABSTRACT.** In the framework of semiclassical theory the universal properties of quantum systems with classically chaotic dynamics can be accounted for through correlations between partner periodic orbits with small action differences. So far, however, the scope of this approach has been mainly limited to systems of a few particles with low-dimensional phase spaces. In the present work we consider  $N$ -particle chaotic systems with local homogeneous interactions, where  $N$  is not necessarily small. Based on a model of coupled cat maps we demonstrate emergence of a new mechanism for correlation between periodic orbit actions. In particular, we show the existence of partner orbits which are specific to many-particle systems. For a sufficiently large  $N$  these new partners dominate the spectrum of correlating periodic orbits and seem to be necessary for construction of a consistent many-particle semiclassical theory.

## 1. MOTIVATION AND GOALS

“Sadly, searching for periodic orbits will never become as popular as a week on Côte d’Azur, or publishing yet another log-log plot in Phys. Rev. Letters.”

— *P. Cvitanović, et al.*, [1]

Already at the dawn of the quantum era it was realized that properties of quantum systems crucially depend on their classical dynamics. While the eigenvalues of integrable systems can be explicitly related to the set of integer numbers by the Bohr-Sommerfeld quantisation rules no such regular structure exists for systems with complex dynamics. At first sight, the energy spectrum of complex systems like nuclei resembles a structureless set of random numbers very much dependent on particularities of the system. This, however, turns out to be not entirely true. The famous Wigner-Dyson-Mehta conjecture asserts that the spectrum of complex quantum systems on the scales of the mean level spacing between eigenvalues is universal and can be described by Random Matrix Ensembles within the same symmetry class. In particular, all  $n$ -point correlation functions of eigenvalues can be derived analytically by using Random Matrix Theory (RMT). Indeed, such spectral statistics have been observed in many real and numerical experiments with various systems ranging from compound nuclei to complex molecules and atoms. Furthermore, it was realized in the early 1980s that even single-particle systems generically exhibit the same universality if their classical dynamics are chaotic. In the last three decades a substantial progress has been achieved in understanding of

the origins of this universality through the application of the semiclassical theory to quantum chaotic systems. In particular, the Gutzwiller's trace formula allows to express eigenvalue density function through the sum of unstable classical periodic orbits. By using this representation the correlations between system eigenenergies can be straightforwardly related to the correlations between actions of periodic orbits. This approach was pioneered by M. Berry in the seminal paper [3], where the diagonal correlations between periodic orbits were taken into account. It was also noted there and in subsequent works [4, 5] that in order to obtain the full RMT result one would need to include non-trivial correlations between periodic orbits as well.

On the quantitative level the non-trivial correlations between periodic orbits were first taken into account in the groundbreaking work of M. Sieber and K. Richter [7]. On the basis of classical chaotic dynamics they demonstrated existence of periodic orbit pairs with close actions. Generally speaking, such orbits traverse approximately the same points of the configuration space but in a different time order. By including the *Sieber-Richter pairs*, and their natural generalizations it turned out to be possible to derive the full RMT result for universal spectral correlations [6].

So far, however, this remarkable progress has by and large been restricted to the systems composed of just few particles. Although, formally Hamiltonian system of  $N$  particles in  $d$  dimensions can be thought as just one particle in  $Nd$  dimension, such dynamical interpretation does not allow to use automatically the “single-particle” semiclassical theory when  $N$  grows simultaneously with  $\hbar^{-1}$ . This is because the standard semiclassical limit assumes a fixed dimensionality of the system while the effective Planck's constant  $\hbar_{eff}$  tends to zero. Another, often considered “semi-classical” theory corresponds to the thermodynamic limit, where  $N \rightarrow \infty$  but  $\hbar_{eff}$  is fixed. As can be clearly seen on the example of bosonic systems, this limit essentially differs from the one where  $N$  is fixed and  $\hbar_{eff} \rightarrow 0$  [10, 11]. Indeed for interacting bosons the two limits correspond to very different classical Hamiltonians associated with the first and the second quantisation of the problem, respectively. At the present, very little is known about the limit where the number of particles  $N$  and the effective dimension  $\hbar_{eff}^{-1}$  of the one-particle Hilbert space grow simultaneously. This is especially frustrating considering that the original Wigner's conjecture relates to many particle systems. One might wonder whether the “single-particle” correlation mechanism between periodic orbits is still relevant for  $N$ -particle chaotic systems. *Do these correlations lead to a spectral universality, when  $N$  is large? At which energy scales? Does the answer depend on the details of the Hamiltonian?*

The central goal of the present paper is to show that  $N$ -particle chaotic systems with local nearest-neighbor interactions allow a more general correlation mechanism between periodic orbit actions than one which is known for one particle systems. By using the one-particle interpretation of classical dynamics it is easy to demonstrate that standard partner orbits (e.g., Sieber-Richter pairs) exist for an arbitrary  $N$ . As expected, these pairs of periodic orbits closely approach each other in the large  $Nd$  dimensional configuration space. It turns out, however, that completely different classes of periodic orbit pairs with close actions exist, as well. In particular, these

non-standard pairs traverse completely different points of the large configuration space. As we show in the body of the paper, they can be interpreted as two-dimensional extensions of standard Sieber-Richter pairs, where periodic orbits sweep surfaces rather than lines in the small configuration space of the corresponding single-particle system. From the semiclassical point of view the contributions from new families of correlating orbits should become dominant over the standard one whenever the number of particles  $N$  exceeds certain threshold value which depends logarithmically on  $\hbar_{eff}^{-1}$ . We believe that in this regime it is essential to take them into account in order to construct a proper semiclassical theory.

The paper is structured in the following order. In the next section we present our main ideas on the heuristic level. The emerging mechanism of correlations between periodic orbits is then discussed in the framework of the particular model of *coupled cat maps*. This model is introduced in Section 3 where we also describe its main dynamical properties. In Section 4 a special duality relation between periodic orbits is introduced. Implications for periodic orbit correlations and few remarkable mathematical identities stemming from this duality are discussed here. In Section 5 we describe general mechanism of correlations between periodic orbits and provide exhausting numerical evidence of its existence. We explicitly construct a number of periodic orbit pairs with small action differences. A general formula for action differences within such pairs of orbits is derived here. The implications of symmetries on the orbit correlations are studied in Section 6. In Section 7 we extend our results to the perturbed maps. Finally, in Section 8 we discuss the relevance of our results for generic many-particle systems with local homogeneous interactions and its implications for a semiclassical quantum theory.

## 2. MAIN IDEAS

In the present work our attention is focused on chaotic systems of  $N$ -particles with local homogeneous interactions. To be more specific, let us write a prototype Hamiltonian which governs the dynamics of suchlike systems:

$$(2.1) \quad \mathcal{H} = \sum_{n=1}^N \frac{p_n^2}{2m} + \mathcal{V}_{\text{in}}(x_n \bmod N, x_{n+1} \bmod N) + \mathcal{V}(x_n).$$

Here  $x_n$  is the particle coordinate belonging to a target space  $\mathcal{X}$  e.g.,  $\mathcal{X} = R^d, S^d$  and  $p_n$  is the corresponding momentum. Since the energy of the system is preserved, the dynamics of (2.1) is restricted to the  $2dN - 1$  energy shell  $\Omega_E$ , determined by the conditions  $\mathcal{H}(x_1 \dots x_N, p_1 \dots p_N) = E$ . Note that  $\mathcal{H}$  is manifestly invariant under the cyclic shift

$$(2.2) \quad \sigma_1 : n \rightarrow n + 1 \bmod N$$

of the particle numbers. In addition to the shift invariance we will assume that the dynamics induced by  $\mathcal{H}$  on  $\Omega_E$  are fully hyperbolic. The last requirement implies that the derivative of the Hamiltonian flow has exactly  $dN - 1$  positive Lyapunov exponents in almost every point of  $\Omega_E$ . Informally speaking, the above Hamiltonian describes a closed string of particles uniformly interacting with their neighbors and

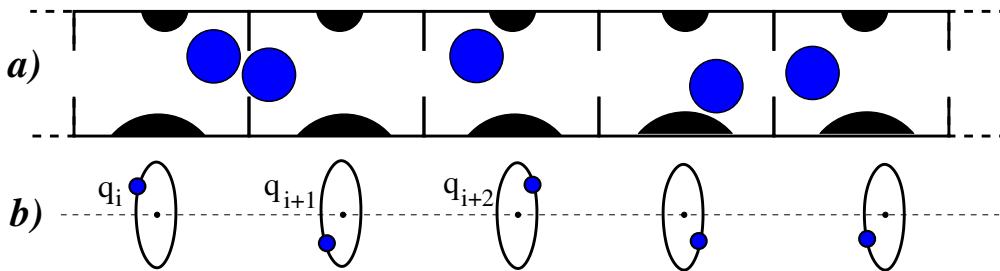


FIGURE 1. In the upper figure (a) is shown the model of Boltzmann gas with the Hamiltonian of the form 2.1. Each ball of the radius  $a$  is constraint to a particular cell of the chain and interacts with the two neighbors through the openings of the size  $L < a$ . On the bottom figure (b) is shown the model of coupled cat map. Each particle lives on a circle of unit length and linearly interacts with the two neighbors at the discrete moments of time. The corresponding time evolution of its coordinate  $q_i$  is described by eq. (3.4).

an external potential  $\mathcal{V}$  such that the resulting dynamics are chaotic. One possible realization of such Hamiltonian is provided by a Boltzmann gas type model shown in fig. 1a.

**Remark 2.1.** *The Hamiltonians of the type (2.1) also appear naturally in connection with the spin chain models and interacting bosons on a circular lattice. For instance, the Bose-Hubbard Hamiltonian written in the second quantisation language:*

$$\hat{\mathcal{H}} = -t \sum_{i=1}^N \hat{b}_i^\dagger \hat{b}_{i+1} + \frac{U}{2} \sum_{i=1}^N \hat{n}_i (\hat{n}_i - 1) - \mu \sum_{i=1}^N \hat{n}_i, \quad \hat{n}_i = \hat{b}_i^\dagger \hat{b}_i$$

can be cast into the form similar to (2.1) after substitution  $\hat{b}_i = \frac{1}{\sqrt{2}}(\hat{x}_i + i\hat{p}_i)$ , where  $\hat{x}_i$  and  $\hat{p}_i$  should be interpreted as the coordinate and the momentum operators of the  $i$ -th harmonic oscillator.

**2.1. Time evolution.** Given some initial conditions the time evolution of a  $N$ -particle system can be represented as collection

$$\Gamma(\tau) = \{\gamma_1(\tau), \gamma_2(\tau), \dots, \gamma_N(\tau)\}, \quad \tau \in \mathbb{R}$$

of one particle trajectories  $\gamma_n(\tau) = (x_n(\tau), p_n(\tau)) \in V$ ,  $n = 1, \dots, N$  in the one-particle  $2d$ -dimensional phase space  $V := T^*\mathcal{X}$ . In what follows we will refer to  $\Gamma(\tau)$  as *many-particle orbit* and as *many-particle periodic orbit* (MPO) if  $\Gamma(\tau)$  is closed i.e.,  $\gamma_n(\tau) = \gamma_n(\tau + \tau_0)$ ,  $n = 1, \dots, N$  after a period  $\tau_0$ . Rather than treating evolution as a continuous flow, it is convenient to discretize dynamics by introducing a discrete Poincaré map acting on a section of the phase space. To this end we fix a Poincaré section  $\mathcal{P}$  which is a  $2dN - 1$  dimensional hypersurface invariant under the shift  $\sigma_1$ , see eq. (2.2), and observe the system at the discrete moments of time  $\tau_t$ ,  $t \in \mathbb{Z}$  when many particle orbit  $\Gamma(\tau)$  pierces  $\mathcal{P}$ . For the system shown in fig. 1a one possible choice for the Poincaré section would be to set it in accordance with the pairwise collisions of the balls. In this case  $\tau_t$  would correspond to the moments of

time when balls collide with each other. The above procedure defines the Poincare map  $\Phi_N$  acting on the  $2dN - 2$  dimensional phase space  $V_N = \mathcal{P} \cap \Omega_E$ , obtained by the intersection of  $\mathcal{P}$  with the energy shell.

Under the action of  $\Phi_N$  any MPO  $\Gamma$  of the system (2.1) can be naturally seen in two different ways. First,  $\Gamma$  can be thought as collection of the points in the  $N$ -particle phase space  $V_N$  registered at the discretized moments of time:

$$\mathcal{S}^1(\Gamma) = \{\Gamma(\tau_1), \Gamma(\tau_2) \dots \Gamma(\tau_T)\}.$$

In other words the evolution of the whole system can be seen as propagation of one particle in the “large” phase space  $V_N$ . Accordingly  $\mathcal{S}^1(\Gamma)$  is naturally interpreted as a discretized one dimensional line. Such a reduction to one particle system is a widely used tool in dynamical systems. For example it allows to treat the Boltzmann gas as a many-dimensional billiard [12].

The second conceptually different way is to look at  $\Gamma$  as a set of  $N \cdot T$  points in the “small” single-particle phase space  $V$ :

$$\mathcal{S}^2(\Gamma) = \{\gamma_{n,t} \mid n = 1, \dots, N, \quad t = 1, \dots, T\},$$

where  $\gamma_{n,t} := \gamma_n(\tau_t)$  marks the position of the  $n$ 'th particle at discrete moment of times  $t = 1, \dots, T$ . For the sake of convenience of presentation it is instructive to introduce the map  $\Psi_\Gamma : \mathbb{Z}_{\text{NT}}^2 \rightarrow V$  which attaches to each point  $(n, t)$  of the discrete “particle-time” space  $\mathbb{Z}_{\text{NT}}^2 := \{1, \dots, N\} \times \{1, \dots, T\}$  the corresponding point  $\gamma_{n,t}$  of the phase space  $V$ . With such notation we have

$$\mathcal{S}^2(\Gamma) = \Psi_\Gamma(\mathbb{Z}_{\text{NT}}^2).$$

In a (properly scaled) continuous limit  $N, T \rightarrow \infty$  the time evolution of the above many-particle system can be seen on an intuitive level as the propagation of a one dimensional closed string  $\gamma(\ell, \tau) = \gamma(\ell + \ell_0, \tau)$ , where  $\ell \in [0, \ell_0]$  measures the length along it and  $\tau$  is continuous time parameter. Accordingly, any periodic orbit of a period  $\tau_0$  can be represented by a two dimensional torus swept by  $\gamma(\ell, \tau)$  in  $V$  during the time  $\tau \in [0, \tau_0]$ . This contrasts with the single-particle interpretation where periodic orbits of the system are naturally represented by one dimensional lines. It should be emphasized that we actually neither require the interaction between particles be attractive nor we consider the continuous limit. So the resulting time evolution of the system might be very different from a string-like motion where all particles keep a linear order in the target space. Nevertheless, regarding the correlation mechanism between periodic orbits it turns out to be quite useful to think about a MPO  $\Gamma$  as of discretized two dimensional surface  $\mathcal{S}^2(\Gamma)$  in the one-particle phase space  $V$  (rather than one dimensional line  $\mathcal{S}^1(\Gamma)$  in the many-particle space  $V_N$ ).

**2.2. One particle partner orbits.** Before focusing on the action correlations between periodic orbits in many-particle systems, let us briefly recall the correlation mechanism in one particle Hamiltonians [6, 7]. A sufficiently long periodic orbit typically has a number of self-encounters. These are the stretches of the trajectory where it closely approaches itself in the configuration space, see fig. 2. For a

trajectory possessing sufficiently long encounters the hyperbolic nature of the dynamics guarantees existence of several (the exact number depends on the encounter structure) of partner periodic orbits which traverse approximately the same points of the phase space, but make different switches at the encounters. The action differences between the partners are accumulated primarily at the encounter stretches and decrease exponentially with their lengths. Accordingly, the periodic orbits of a hyperbolic system can be organized into families, where all members have approximately the same actions.

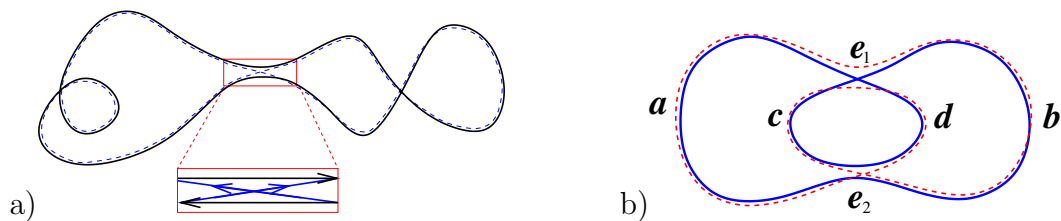


FIGURE 2. On the left is shown the caricature of a Sieber-Richter pair with one encounter shown as a (red) box. Such partner orbits exist only in systems with time reversal symmetry. On the right it is shown the caricature of a periodic orbit (solid line) and its partner (dashed line) with two encounters  $e_1$ ,  $e_2$ . Their symbolic representations are given by (2.3).

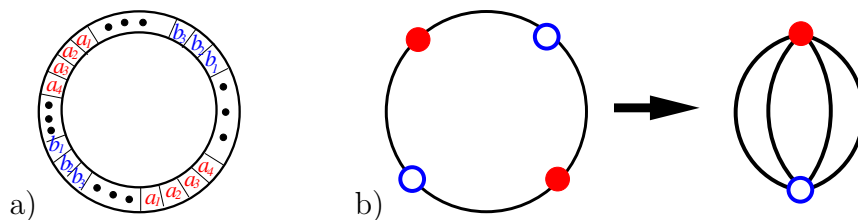


FIGURE 3. a) Schematic depiction of 1D symbolic representation of the periodic orbit on fig. 2b. Two encounter regions correspond to the identical sequences of symbols labeled by  $a$  and  $b$  letters respectively b) The structural diagram of the same periodic orbit. The encounter regions correspond to two pairs of points on the circle  $T^1$ . After “gluing” the circle at these points we obtain the graph shown in the second figure. This graph can be also interpreted as Feynman diagram for a zero-dimensional sigma model which describes universal spectral correlations in quantum systems with classically chaotic dynamics, see [6].

**2.2.1. Symbolic dynamics.** The intuitive description of the above correlation mechanism between periodic orbits can be formalized by making use of symbolic dynamics [14, 15]. Within this approach the first step is to fix a Poincare section and consider the discretized time evolution. Assuming that the reduced phase space of the system allows a finite Markov partition  $\bigsqcup_{\alpha \in \mathcal{A}} V_\alpha$ , any trajectory  $\gamma$  can be encoded by a doubly infinite sequence of symbols from some alphabet  $\mathcal{A}$  of a finite size:

$$\dots a_{-2}a_{-1}a_0.a_1a_2\dots$$

Here each symbol  $a_t$  registers the position of the particle with respect to the partition at the discrete time  $t$ , i.e.,  $a_t$  equals to  $\alpha \in \mathcal{A}$  if  $\gamma(t) \in V_\alpha$ . Correspondingly, a  $n$ -periodic orbit  $\gamma$  can be associated with a cyclic sequence of the length  $n$ :

$$a_\gamma = [a_1 a_2 \dots a_n], \quad a_i \in \mathcal{A}.$$

On the level of symbolic dynamics each  $l$ -*encounter* of the length  $p$  in  $\gamma$  is a string of  $p$  symbols  $e = \epsilon_1 \epsilon_2 \dots \epsilon_p$  which appears in  $a_\gamma$  a number  $l > 1$  of times, see fig. 3a. Given a periodic sequence  $a_\gamma$  its pair sequence  $a_{\bar{\gamma}}$  is constructed by rearranging the encounters and stretches of symbols connecting them in a way that any subsequence of consecutive  $p$  symbols existing in  $a_\gamma$  reappears in  $a_{\bar{\gamma}}$  exactly the same number of times and vice versa. Since the approximate position of a point in the phase space is determined by a finite string of symbols, the above property guarantees that the corresponding orbits traverse approximately the same points of the phase space. For instance, the following two sequences:

$$(2.3) \quad a_\gamma = [ae_1 de_2 ce_1 be_2], \quad a_{\bar{\gamma}} = [ae_1 be_2 ce_1 de_2],$$

with the encounters  $e_1, e_2$  of some length  $p$  and stretches  $a, b, c, d$  of an arbitrary length connecting them provide the symbolic representation of partner orbits shown on fig. 2b.

Structurally different families of partner orbits  $\{\gamma\}$  can be distinguished by their diagrams  $\mathcal{F}_\gamma$  accounting for different order of encounters. Each of the diagrams is obtained by substituting encounters of  $\gamma$  with the points and placing them (in the same linear order) on a circle  $T^1$ . The points belonging to the same encounters are then identified (i.e.,  $T^1$  is “glued” to itself at these points), see fig. 3b. The resulting graph  $\mathcal{F}_\gamma$  carries all structural information on the correlations between the partner orbits  $\{\gamma\}$ . In particular, it defines the number of partner orbits within the family. It worth mentioning that in the semiclassical theory based on the correlations between periodic orbits such graphs can be associated with Feynman diagrams of the corresponding sigma model [6].

**2.3. Many particle partner orbits.** We turn now our attention to the  $N$ -particle systems with the local type of interactions (2.1). At the beginning of this section we argued that in the limit of continuous  $N$  the periodic orbits of such a system can be regarded as two-dimensional surfaces in the phase space. Taking this as a guiding principle let us first analyze on an intuitive level its implications on the correlation mechanism between periodic orbit actions. By the analogy with the single-particle case, we demand that the two surfaces corresponding to some pair of partner periodic orbits  $\Gamma, \bar{\Gamma}$  pass through approximately the same points of the phase space i.e.,

$$S^2(\Gamma) = \Psi_\Gamma(\mathbb{Z}_{\text{NT}}^2) \approx \Psi_{\bar{\Gamma}}(\mathbb{Z}_{\text{NT}}^2) = S^2(\bar{\Gamma}).$$

For this to happen each periodic orbit must have at least one  $l$ -encounter, which is an element of the configuration space where the surface approaches itself sufficiently closely for a number  $l \geq 2$  times, see fig. 4. The existence of the encounter implies that there are  $l$  disjoint domains  $E^{(i)} \subset \mathbb{Z}_{\text{NT}}^2, i = 1, \dots, l$  related to each other by

the translation shift  $\sigma_2^{(n',t')}: (n, t) \rightarrow (n + n' \bmod N, t + t' \bmod T)$ :

$$(2.4) \quad E^{(i)} = \sigma_2^{(n_i, t_i)} \cdot E^{(1)}, \text{ for } i = 1, \dots, l, \quad E^{(i)} \cap E^{(j)} = \emptyset, \text{ for } i \neq j$$

such that all domains are mapped into approximately the same points of the target space  $V_N$ :

$$\Psi_\Gamma(E^{(1)}) \approx \Psi_\Gamma(E^{(2)}) \approx \dots \approx \Psi_\Gamma(E^{(l)}) \approx \Psi_{\bar{\Gamma}}(E^{(1)}) \approx \Psi_{\bar{\Gamma}}(E^{(2)}) \approx \dots \approx \Psi_{\bar{\Gamma}}(E^{(l)}).$$

Conversely, whenever a closed surface possesses encounters it might be possible to find a pair surface traversing almost the same points of the phase space. Therefore, the problem of classifying structurally different families of correlating MPOs can be on a geometrical level understood as one of finding all topologically non-equivalent ways to “glue” a two-dimensional surface to itself. This is very much similar to the single-particle case where we need to classify the non-trivial ways to “glue” one-dimensional lines.

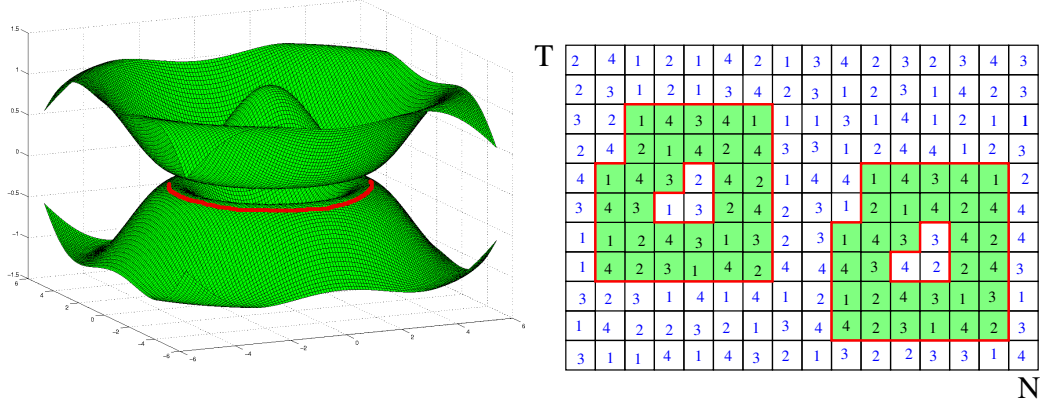


FIGURE 4. On the left is a geometric representation of MPO with an encounter (shown in red). On the right is shown symbolic representation of suchlike MPO. Here the alphabet is composed of four symbols  $\{1, 2, 3, 4\}$ . The encounter region is encoded by 2D sequence of symbols (shown in green) which reappears in two different places of  $\mathbb{Z}_{NT}^2$ . (color on line)

**2.3.1. 2D symbolic representation.** The above intuitive geometrical picture of partner MPOs can be made precise through introduction of two dimensional (2D) symbolic dynamics. Within this approach, it is assumed that each many particle (periodic) orbit  $\Gamma$  can be encoded by a two dimensional (periodic) lattice of symbols  $a_{n,t}$ ,  $(n, t) \in \mathbb{Z}^2$ , where symbols  $a_{n,t}$  belong to some alphabet  $\mathcal{A}$  of a small size. Naturally, each MPO  $\Gamma$  is represented then by  $N \times T$  toroidal array of symbols:

$$\mathbb{A}_\Gamma = \{a_{n,t} \mid (n, t) \in \mathbb{Z}_{NT}^2\}.$$

**Remark 2.2.** One formal way to construct such a symbolic representation, would be to use some partition  $\bigsqcup_{\alpha \in \mathcal{A}} V_\alpha$  of the one-particle phase space  $V$ . At a time  $t$  a symbol  $a_{n,t} \in \mathcal{A}$  is attached to the  $n$ 'th particle, if the point  $\gamma_{n,t}$  belongs to the corresponding part of the partition:  $V_{a_{n,t}}$ . A symbolic representation of this type has



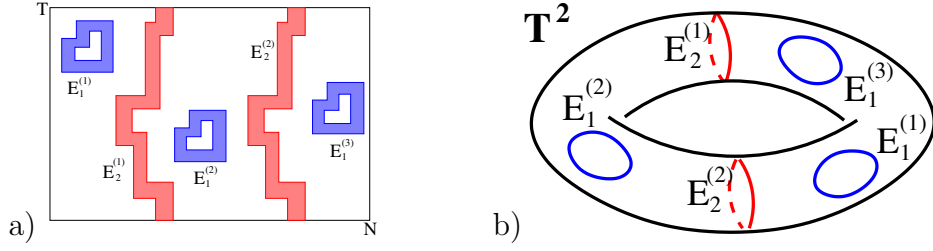


FIGURE 5. a) Schematic depiction of 2D symbolic representation for a MPO  $\Gamma$  with two encounters. The first 3-encounter has winding numbers  $(0,0)$ . It is represented by three identical sets of symbols at the frame-like domains  $E_1^{(i)}$ ,  $i = 1, 2, 3$  shifted with respect to each other on the torus  $\mathbb{Z}_{NT}^2$ . The second 2-encounter is represented by two identical sets of symbols at the strip-like domains  $E_2^{(i)}$ ,  $i = 1, 2$  and has winding numbers  $(0,1)$ . b) The structural diagram  $\mathcal{F}_\Gamma$  of the MPO on the left figure. The two encounter regions correspond here to 3 identical (blue) oval lines and 2 (red) lines winding around the torus. The two-dimensional surface  $\mathcal{F}_\Gamma$  is obtained by “gluing” the torus along the identical lines. Compare with the one particle structural diagram shown in fig. 3.

been constructed for a model of coupled lattice maps in [22]

To facilitate further discussion we introduce the map  $\psi_\Gamma : \mathbb{Z}_{NT}^2 \rightarrow \mathcal{A}$  which assigns to each point  $(n, t) \in \mathbb{Z}_{NT}^2$  the corresponding symbolic representation  $a_{n,t}$  of  $\Gamma$  i.e.,

$$\psi_\Gamma(n, t) = a_{n,t}.$$

In what follows the array  $\mathbb{A}_\Gamma \equiv \psi_\Gamma(\mathbb{Z}_{NT}^2)$  is referred to as 2D symbolic representation of  $\Gamma$ . By the analogy with one-dimensional symbolic dynamics of hyperbolic systems we require few basic properties for such 2D encoding.

- *Small alphabet*: The number of symbols in  $\mathcal{A}$  is independent of  $N$ .
- *Locality*: The symbols in a neighborhood of each point  $(n, t)$  define an approximate position in the phase space of the  $n$ 'th particle at the time  $t$ . More precisely, let  $p$  be an odd integer and let

$$\mathcal{R}_p^{(n,t)} = \{(i, j) | i = n - (p-1)/2 \bmod N, \dots, n + (p-1)/2 \bmod N, \\ j = t - (p-1)/2 \bmod T, \dots, t + (p-1)/2 \bmod T\}$$

be a square-like set of  $p \times p$  points around  $(n, t)$ . We require that for any two MPOs  $\Gamma = \{\gamma_{n,t} | (n, t) \in \mathbb{Z}_{NT}^2\}$ ,  $\Gamma' = \{\gamma'_{n,t} | (n, t) \in \mathbb{Z}_{NT}^2\}$  having the same symbolic representation at the set  $\mathcal{R}_p^{(n,t)}$  i.e.,  $\psi_\Gamma(\mathcal{R}_p^{(n,t)}) = \psi_{\Gamma'}(\mathcal{R}_p^{(n,t)})$ , the distance between the corresponding points in the phase space is bounded in an exponential way:

$$(2.5) \quad |\gamma_{n,t} - \gamma'_{n,t}| < \Lambda^{-p},$$

where  $\Lambda$  is some constant.

- *Uniqueness*: For each MPO there is a unique 2D symbolic representation. In other words if  $\psi_\Gamma(\mathbb{Z}_{\text{NT}}^2) = \psi_{\Gamma'}(\mathbb{Z}_{\text{NT}}^2)$ , then necessarily  $\Gamma = \Gamma'$ . Note that we do not require the opposite i.e., there might be 2D sequences of symbols which do not correspond to any real MPO.

Whether or not there exists symbolic representation of periodic orbits with the above properties is a highly non-trivial question, which should be, in principle, explored for each system individually. It is known that such 2D symbolic representation can be constructed for some coupled lattice maps [22]. In the body of the paper we also demonstrate the existence of suchlike symbolic dynamics for the model of coupled cat maps. Leaving for a while the problem of existence aside let us describe how the 2D symbolic representation can be utilized in order to find partner MPOs.

**2.3.2. Partner orbits.** First recall that by definition partner MPOs  $\Gamma, \bar{\Gamma}$  pass through approximately the same points of the phase space. The locality property of the symbolic dynamics implies that the symbolic representation  $\mathbb{A}_\Gamma$  in a neighborhood of a point  $(n, t)$  must coincide with one of its partner  $\mathbb{A}_{\bar{\Gamma}}$  in the neighborhood of some another point  $(\bar{n}, \bar{t})$ . This motivates the following definition.

**Definition 2.3.** *Let  $p$  be a fixed positive integer. We call two symbolic representations  $\mathbb{A}_\Gamma, \mathbb{A}_{\bar{\Gamma}}$  as  $p$ -close iff any  $p \times p$  square of symbols:*

$$(2.6) \quad [\alpha]_p = \begin{pmatrix} \alpha_{1,1} & \alpha_{1,2} & \dots & \alpha_{1,p} \\ \alpha_{2,1} & \alpha_{2,2} & \dots & \alpha_{2,p} \\ \vdots & \vdots & \ddots & \vdots \\ \alpha_{p,1} & \alpha_{p,2} & \dots & \alpha_{p,p} \end{pmatrix}, \quad \alpha_{i,j} \in \mathcal{A}$$

*appears the same number of times (which might be also zero) in both  $\mathbb{A}_\Gamma$  and  $\mathbb{A}_{\bar{\Gamma}}$ .*

Clearly if two MPOs  $\Gamma, \bar{\Gamma}$  have  $p$ -close 2D symbolic representations  $\mathbb{A}_\Gamma, \mathbb{A}_{\bar{\Gamma}}$  then  $\Gamma$  and  $\bar{\Gamma}$  are partner orbits, with the parameter  $p$  controlling how close the sets  $S^2(\Gamma), S^2(\bar{\Gamma})$  approach each other in the phase space.

Given a 2D symbolic representation  $\mathbb{A}_\Gamma$  a  $p$ -close 2D sequence might only exist if  $\mathbb{A}_\Gamma$  contains at least one  $l$ -encounter of a “width”  $p$ . In other words, if  $\Gamma$  has a partner orbit  $\bar{\Gamma}$  there exist  $l$  disjoint domains  $E^{(i)} \subset \mathbb{Z}_{\text{NT}}^2, i = 1, \dots, l$  satisfying (2.4) such that 2D subsequences of symbols at all  $E^{(i)}$  coincide (see fig. 4):

$$(2.7) \quad \psi_\Gamma(E^{(1)}) = \psi_\Gamma(E^{(2)}) = \dots = \psi_\Gamma(E^{(l)}).$$

A general encounter region can be defined by fixing closed (translationally related) discrete line contours  $\mathcal{T}_{E^{(i)}}, i = 1, \dots, l$  and expanding them into “strips” of finite width. The resulting sets  $E_i, i = 1, \dots, l$  must fulfill the eq. (2.4) and satisfy the following two requirements: 1) The interior of each  $\mathcal{T}_{E^{(i)}}$  should contain at least one point which does not belong to  $E^{(i)}$  i.e.,  $E^{(i)}$  has to be multi-connected. 2) For any  $(n, t) \in \mathcal{T}_{E^{(i)}}$  one has  $\mathcal{R}_p^{(n,t)} \subseteq E^{(i)}$ . Structurally different encounters can be distinguished by their winding numbers  $w = (w_1, w_2)$  specifying how many times the path  $\mathcal{T}_{E^{(i)}}$  goes around the torus  $\mathbb{Z}_{\text{NT}}^2$  in the particle and the time directions, respectively.

Let  $\Gamma$  be a MPO and let  $\mathbb{A}_\Gamma$  be its symbolic representation. In general  $\Gamma$  might contain a number  $\mathcal{N}$  of encounters with different multiplicities  $l_n$  and winding numbers  $w_n$ ,  $n = 1, \dots, \mathcal{N}$ . For each encounter there exist  $l_n$  corresponding sets of points  $E_n^{(i)} \subset \mathbb{Z}_{\text{NT}}^2$ ,  $i = 1, \dots, l_n$  related by shift translation such that symbolic representation of  $\Gamma$  on all these sets coincide, see fig. 5a. To distinguish between different classes of MPOs let us introduce for each  $\Gamma$  the corresponding diagram  $\mathcal{F}_\Gamma$  keeping the topological information about its encounters structure. To this end substitute  $\mathbb{Z}_{\text{NT}}^2$  with a 2-dimensional torus  $T^2$  and each set  $E_n^{(i)}$  with a line  $\gamma_n^{(i)} \subset T^2$  (whose exact shape of no importance) having the same winding numbers and the same geometrical order as the corresponding encounters. We then identify the points of  $T^2$  which belong to the lines  $\gamma_n^{(i)}$ ,  $i = 1, \dots, l_n$ , see fig. 5b. (Informally speaking, we glue the torus to itself along the lines from the same encounter). The resulting surface  $\mathcal{F}_\Gamma$  will be referred to as *structural diagram* of  $\Gamma$ . It has the the same role as the structural graph for one-particle periodic orbits, see fig. 3. In particular,  $\mathcal{F}_\Gamma$  defines the number of  $\Gamma$ 's partners.

The symbolic representation  $\mathbb{A}_{\bar{\Gamma}}$  of a partner orbit  $\bar{\Gamma}$  of  $\Gamma$  can be recovered from  $\mathbb{A}_\Gamma$  by exchanging the patches of symbols outside the encounter regions. The exact rules for such exchange and the number of partner orbits obtained in this way depend only on the structural diagram  $\mathcal{F}_\Gamma$  of the MPO. Below we illustrate this procedure for periodic orbits with the minimal possible number (one and two) of 2-encounters having winding numbers:  $w = (0, 1)$ ,  $w = (1, 0)$  and  $w = (0, 0)$ . As will be argued in Section 8, MPOs with such encounters are the most relevant from the semiclassical point of view.

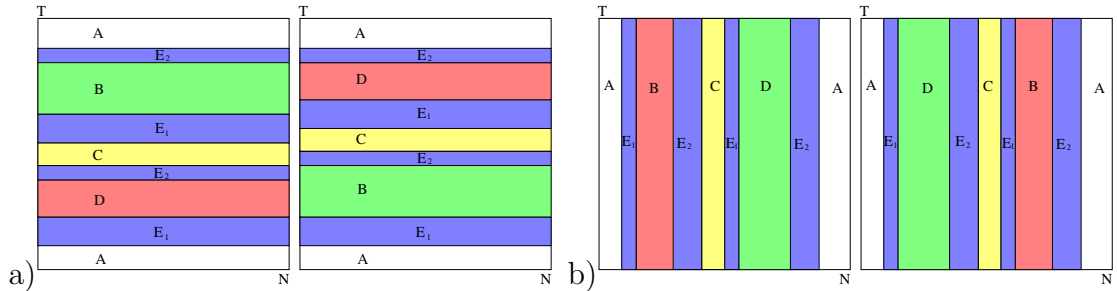


FIGURE 6. On the left figure (a) are shown two partner MPOs with two encounters winding around the torus  $\mathbb{Z}_{\text{NT}}^2$  in the particle direction. The 2D symbolic representation of the second MPO is obtained from the first one by exchanging symbols in the domains  $B$  and  $D$ . In one particle interpretation this is precisely the pair of trajectories shown in fig. 2b. On the right figure (b) are shown two partner orbits with encounters winding around the torus in the time direction. Their construction is precisely the same as on the left figure with the switched particle and time directions.

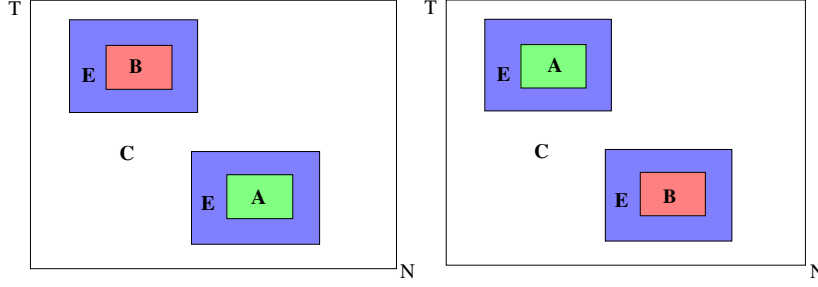


FIGURE 7. The pair of MPOs with one encounter having zero winding numbers. The 2D symbolic representation of the second MPO (right) is obtained from the first one (left) by exchanging symbols in the domains  $A$  and  $B$ .

**a) “Horizontal” encounters:**  $w = (1, 0)$ . Encounters of this type wind up torus in the particle direction. A simple example is provided by the two horizontal strips:

$$E = \{t_1, \dots, t_1 + p\} \times \{1, \dots, N\}, \quad E' = \{t_2, \dots, t_2 + p\} \times \{1, \dots, N\},$$

$|t_2 - t_1| > p \in \mathbb{N}$ , with the symbolic sequences coinciding on these sets:

$$E = \psi_\Gamma(E) = \psi_\Gamma(E').$$

If  $\Gamma$  has two such encounters with the symbolic representations  $E_1$  and  $E_2$ , respectively the symbolic representation of its partner  $\bar{\Gamma}$  can be constructed simply by using the same procedure as in the single-particle case, see eq. (2.3) and fig. 6a.

**b) “Vertical” encounters:**  $w = (0, 1)$ . These encounters wind up around torus in the time direction. For instance the following pair of vertical strips

$$E = \{1, \dots, T\} \times \{n_1, \dots, n_1 + p\}, \quad E' = \{1, \dots, T\} \times \{n_2, \dots, n_2 + \Delta n\},$$

$|n_2 - n_1| > p \in \mathbb{N}$  carrying the same symbolic representation defines an encounter with the required winding numbers. The construction of partner orbits here is completely analogous to the previous case up to the switch between particle and time directions, see fig. 6b.

**c) “Annular” encounters:**  $w = (0, 0)$ . For the construction of partner orbits in this case, it is sufficient to have a periodic orbit with just one encounter. Let  $A$  and  $B$  be two sets of the points from  $\mathbb{Z}_{\text{NT}}^2$  corresponding to the interiors of the encounter sets  $E, E'$ , as shown in fig. 7. If  $\mathbb{A}_\Gamma$  is the symbolic representation of MPO  $\Gamma$ , the symbolic representation  $\mathbb{A}_{\bar{\Gamma}}$  of its partner orbit  $\bar{\Gamma}$  is obtained by exchanging the symbols  $A = \psi_\Gamma(A)$  with  $B = \psi_\Gamma(B)$ , see fig. 7.

**2.4. Comparison between one-particle and  $N$ -particle partner orbits.** Recall that a MPO might have a partner orbit only if it poses an encounter. What does the existence of an encounter in  $N$ -particle systems implies on the level of individual particles? Regarding a MPO as single-particle closed orbit in many-dimensional phase space the standard definition of encounter would imply that all particles simultaneously reappear at (approximately) the same positions at least twice during the period of motion. This is indeed the correct interpretation for horizontal type of encounters having winding numbers  $(1, 0)$ . However, encounters with other winding

numbers have a different interpretation in the many particle systems (2.1). For instance, if the two encounter domains have the shapes of horizontal strips, see fig. 6b, only a number of the particles  $n_1, n_1 + 1, \dots, n_1 + p$  perform approximately the same motion in  $V$  as the particles  $n_2, n_2 + 1, \dots, n_2 + p$ , but they do it for all times between 0 and  $T$ . Furthermore, having an encounter of an annular type shown in fig. 7 implies that a group of particles retrace positions of another group of particles in a different point of time. We would like to emphasize that only the horizontal strips which wrap the torus in the particle direction would qualify as encounters in the one particle interpretation. So the 2D representation of MPOs is absolutely necessary in order to account for partner orbits with other types of encounters.

So far the whole discussion of the correlation mechanism between MPOs has been restricted to a pure conceptual level. In the next section we introduce a particular model of the type (2.1). Within this model we are able to demonstrate existence of the partner MPOs and estimate the differences between their actions.

### 3. MODEL OF COUPLED CAT MAPS

From the technical point of view it is often convenient to consider dynamical systems whose time evolution is given from the start by a discrete map rather than by a continuous flow. One of the best studied and understood examples of systems with chaotic dynamics are provided by *cat maps* which are the hyperbolic automorphisms of the unit 2-torus  $V = T^2$  [20, 16]. To introduce a many particle set up we couple  $N$  cat maps in a linear way, such that the resulting  $2N$  dimensional map:

$$\Phi_N : V_N \rightarrow V_N, \quad V_N = \underbrace{T^2 \times T^2 \dots \times T^2}_N$$

is again a hyperbolic automorphism of the unit  $2N$ -torus  $V_N \cong T^{2N}$ , see fig. 1. Specifically, the generating function of the map  $\Phi_N$  is defined as

$$(3.1) \quad S(\mathbf{q}_t, \mathbf{q}_{t+1}) = d \sum_{n=1}^N q_{n,t} q_{1+(n \bmod N),t} + c \sum_{n=1}^N q_{n,t} (q_{n,t+1} + m_{n,t+1}^q) + \\ + \frac{a}{2} \sum_{n=1}^N q_{n,t}^2 + \frac{b}{2} \sum_{n=1}^N (q_{n,t+1} + m_{n,t+1}^q)^2 - m_{n,t+1}^p q_{n,t+1} + \mathcal{V}(q_{n,t}),$$

where  $\mathbf{q}_t = \{q_{n,t}\}_{n=1}^N$ , with  $q_{n,t}$  being the coordinate of  $n$ -th particle  $n = 1 \dots N$  at the moment of time  $t \in \mathbb{Z}$ , and  $m_{n,t+1}^q, m_{n,t+1}^p$  are integer numbers which stand for winding numbers along the  $q$  and  $p$  directions of the  $2N$ -torus. The coefficients  $a, b, c, d$  are constants which will be specified below and  $\mathcal{V}(q)$  is a smooth periodic function  $\mathcal{V}(q+1) = \mathcal{V}(q)$ . In the following we refer to the map generated by the action (3.1) as non-perturbed (resp. perturbed) *coupled cat map* in the case when  $\mathcal{V}(q) = 0$  (resp.  $\mathcal{V}(q) \neq 0$ ).

The map  $\Phi_N$  shares the most important properties with the model (2.1). In particular, it is defined in such a way that all particles are coupled in a uniform way with its nearest neighbors. Models of this type are known as coupled lattice

maps. Their dynamical properties have been extensively studied in the last three decades [21]. Of special interest for us, is the result from [22], where existence of 2D symbolic dynamics was demonstrated for a particular model of coupled lattice map. In the following we show that 2D symbolic dynamics with the properties described in Section 2.3.1 can be constructed also for the map  $\Phi_N$ .

**3.1. Dynamics.** The equation of motion is generated using  $p_{n,t} = -\partial S/\partial q_{n,t}$ ,  $p_{n,t+1} = \partial S/\partial q_{n,t+1}$ :

$$(3.2) \quad \begin{aligned} q_{n,t+1} &= \frac{1}{c}(-p_{n,t} - a q_{n,t}) - \frac{d}{c}(q_{n+1,t} + q_{n-1,t}) - m_{n,t+1}^q - \frac{1}{c}\mathcal{V}'(q_{n,t}) \\ p_{n,t+1} &= \frac{1}{c}(-b p_{n,t} + (c^2 - ab)q_{n,t}) - \frac{db}{c}(q_{n+1,t} + q_{n-1,t}) - m_{n,t+1}^p - \frac{b}{c}\mathcal{V}'(q_{n,t}). \end{aligned}$$

Under the condition that  $\mathcal{V}(q) = 0$  these equations can also be written in the matrix form:

$$Z_{t+1} = \mathfrak{B}_N Z_t \mod 1, \quad Z_t = (q_{1,t}, p_{1,t}, \dots, q_{N,t}, p_{N,t})^T,$$

with  $2N \times 2N$  matrix  $\mathfrak{B}_N$  given by:

$$(3.3) \quad \mathfrak{B}_N = \begin{pmatrix} A & B & \mathbf{0} & \dots & \mathbf{0} & B \\ B & A & B & \dots & \mathbf{0} & \mathbf{0} \\ \mathbf{0} & B & A & \dots & \mathbf{0} & \mathbf{0} \\ \vdots & \vdots & \vdots & \ddots & \vdots & \vdots \\ \mathbf{0} & \mathbf{0} & \mathbf{0} & \dots & A & B \\ B & \mathbf{0} & \mathbf{0} & \dots & B & A \end{pmatrix},$$

$$A = -\frac{1}{c} \begin{pmatrix} a & 1 \\ ab - c^2 & b \end{pmatrix}, \quad B = -\frac{1}{c} \begin{pmatrix} d & 0 \\ db & 0 \end{pmatrix}.$$

For the map to be continuous the elements of the matrix  $\mathfrak{B}_N$  must be integers. To satisfy this requirement we set  $c = -1$  and  $a, b, d \in \mathbb{Z}$ .

By excluding the momentum from the system of eqs. (3.2) the dynamical equations for the time evolution can be cast into the Newtonian form:

$$(3.4) \quad \begin{aligned} c(q_{n,t+1} + q_{n,t-1}) + d(q_{n+1,t} + q_{n-1,t}) &= -(a+b)q_{n,t} + m_{n,t} - \mathcal{V}'(q_{n,t}), \\ m_{n,t} &= -b m_{n,t}^q - c m_{n,t+1}^q + m_{n,t}^p. \end{aligned}$$

**3.2. Spectrum of  $\mathfrak{B}_N$ .** In order to establish the type of dynamics generated by  $\Phi_N$  we need to determine the spectrum of the matrix  $\mathfrak{B}_N$ . Since  $\mathfrak{B}_N$  is a circular matrix which commutes with the shift operator its spectrum can be found explicitly. After substitution  $\bar{Z} = (\bar{q}_1, \bar{p}_1, \dots, \bar{q}_N, \bar{p}_N)$  into the spectral equation

$$\lambda \bar{Z} = \mathfrak{B}_N \bar{Z}$$

we obtain the following condition

$$\gamma \bar{q}_n = \bar{q}_{n+1} + \bar{q}_{n-1}, \quad d\gamma = -s + \lambda + \frac{1}{\lambda}, \quad s = a + b,$$

which is equivalent to the iterative equation:

$$(3.5) \quad \begin{pmatrix} \bar{q}_{n+1} \\ \bar{q}_n \end{pmatrix} = \begin{pmatrix} \gamma & -1 \\ 1 & 0 \end{pmatrix} \begin{pmatrix} \bar{q}_n \\ \bar{q}_{n-1} \end{pmatrix}.$$

In order to close this equation the eigenvalue of the matrix above must be of the form  $e^{2\pi i k/N}$ ,  $k = 1, \dots, N$ . This yields to the following quadratic equation for eigenvalues of  $\mathfrak{B}_N$ :

$$(3.6) \quad \lambda + \lambda^{-1} = s + 2d \cos(2\pi k/N), \quad k = 1, \dots, N.$$

Accordingly,  $\Phi_N$  is fully hyperbolic iff  $|s| > 2|d| + 2$ . In this case all solutions  $\lambda_{\pm}(k)$  of this equation are paired such that  $\lambda_+(k) = \lambda_-^{-1}(k)$  and  $|\lambda_+(k)| > 1$  for all  $k$ . In what follows we will assume that this condition is always satisfied.

**3.3. Periodic orbits.** In this paper we primarily focus on the periodic orbits of  $\Phi_N$ . In the case of fully hyperbolic dynamics the total number  $\mathcal{N}(T)$  of MPO with period  $T$  can be easily obtained by the following formula:

$$(3.7) \quad \mathcal{N}(T) = |\det(I - \mathfrak{B}_N^T)| \approx \prod_{k=1}^N \lambda_+^T(k),$$

where  $\lambda_+(k)$  are solutions of eq. (3.6) with the largest absolute value. It is straightforward to see that  $\mathcal{N}(T)$  grows exponentially both with  $N$  and  $T$ .

The action of periodic orbits can be, in principle, obtained by summing up all the terms in eq. (3.1) along the trajectory. Note, however that the generating function  $S(\mathbf{q}_t, \mathbf{q}_{t+1})$  also contains half-integer factors  $b(m_{n,t}^q)^2/2$  which are in fact irrelevant, as far as, the dynamical equations of concern. For convenience we omit these factors from the definition of actions. Such omission also does not affect the semiclassical theory, where only a fractional part of the actions plays a role, see e.g., [16, 19]. Accordingly if  $\Gamma$  is a MPO with a period  $T$ , its action is defined by:

$$(3.8) \quad S_{\Gamma} = \sum_{t=1}^T \sum_{n=1}^N \left( dq_{n,t} q_{1+(n \bmod N),t} + c q_{n,t} q_{n,t+1} + \frac{a}{2} q_{n,t}^2 + \frac{b}{2} q_{n,t+1}^2 + \mathcal{V}(q_{n,t}) \right) + \\ + \sum_{t=1}^T \sum_{n=1}^N (c q_{n,t} m_{n,t+1}^q + b q_{n,t+1} m_{n,t+1}^q - m_{n,t+1}^p q_{n,t+1}),$$

where  $q_{n,t}, m_{n,t}^{(q,p)}$ , are coordinates and winding numbers along  $\Gamma$ . Using eq. (3.4) this expression can be further simplified leading to:

$$(3.9) \quad S_{\Gamma} = -\frac{1}{2} \sum_{t=1}^T \sum_{n=1}^N m_{n,t} q_{n,t} + q_{n,t} \mathcal{V}'(q_{n,t}) - 2\mathcal{V}(q_{n,t})$$

**Remark 3.1.** *It worth mentioning that in most of the works on cat maps the actions of periodic orbits are defined in a somewhat different way, see e.g., [16]. Namely, if a periodic orbit  $\Gamma$  has a period  $T$  one looks for a fixed point  $(\mathbf{q}, \mathbf{p})$  of the map  $\Phi_N^T$ , and then defines the action of  $\Gamma$  as  $\tilde{S}_{\Gamma}(\mathbf{q}) = S(\mathbf{q}, \mathbf{q})$ , where the generating function  $S$  is given by eq. (3.1) with the parameters  $a, b, c, d$  defined by the map  $\Phi_N^T$ , rather*

then by  $\Phi_N$ . It can be shown that the difference between two actions  $\tilde{S}_\Gamma$  and  $S_\Gamma$  is always an integer. Since in quantum mechanics only fractional part of actions are of a relevance one can use both definition equivalently for semiclassical calculations. We, however believe that (3.9) is a more natural one from a classical point of view as its properties resemble ones of periodic orbit actions in generic Hamiltonian systems. Note, that in contrast to  $S_\Gamma$ ,  $\tilde{S}_\Gamma(\mathbf{q})$  depends on the choice of the initial point  $\mathbf{q}$  at  $\Gamma$  i.e.,  $\tilde{S}_\Gamma(\mathbf{q}) \neq \tilde{S}_\Gamma(\Phi_N \cdot \mathbf{q})$  and it grows exponentially with  $T$ .

#### 4. TIME-PARTICLE DUALITY

Remarkably, for  $c = d$  the equation (3.4) becomes symmetric under the exchange of times and particle numbers:  $n \leftrightarrow t$ . This immediately leads to the following duality relationship between periodic orbits of the system.

**Lemma 4.1.** *Let  $\Phi_k$  be a sequence of maps (3.1) with some fixed parameters  $a, b, c = d$  and varied number of particles  $k = 1, 2, \dots$ . For each MPO  $\Gamma$  of  $\Phi_N$  with a period  $T$  there exists corresponding MPO  $\Gamma'$  of the map  $\Phi_T$  with the period  $N$ , such that both trajectories run through the same set of points in the configuration space. Furthermore, the actions of two orbits coincide  $S_\Gamma = S_{\Gamma'}$ .*

*Proof:* The proof is straightforward. Given a MPO  $\Gamma$  the set of points  $\{q_{n,t}, m_{n,t} | n = 1, \dots, N; t = 1, \dots, T\}$  traversed by  $\Gamma$  in the configuration space must satisfy eq. (3.4). By defining  $q_{n,t} = q'_{t,n}$ ,  $m_{n,t} = m'_{t,n}$  one can easily see that the new set  $\{q'_{n,t}, m'_{n,t} | n = 1, \dots, T; t = 1, \dots, N\}$  satisfies eq. (3.4), as well. It remains to notice that the set  $\{q'_{n,t}, m'_{n,t}\}$  uniquely defines the trajectory  $\Gamma'$  of the period  $N$  for the map  $\Phi_T$ . The equality between actions then follows immediately from eq. (3.8).  $\square$

**Remarks 4.2.** 1) The above lemma holds also for the case of perturbed cat maps when  $\mathcal{V}(q) \neq 0$ . 2) Note that although the two trajectories  $\Gamma, \Gamma'$  traverse the same points of the configuration space, they do not have the same set of momenta. 2) For  $N = T$  the set of periodic trajectories becomes self-dual. This means that each MPO  $\Gamma$  either has a pair MPO  $\Gamma'$  satisfying  $q_{n,t} = q'_{t,n}$  or satisfies the self-dual constraint  $q_{n,t} = q_{t,n}$  for each  $t$  and  $n$ . The first option would actually imply that  $\Gamma$  and  $\Gamma'$  traverse through exactly the same points of the configuration space. We have not observed such pairs in our numerical simulations.

An immediate consequence of this lemma is the following connection between numbers of periodic orbits.

**Lemma 4.3.** *The number of MPOs with a period  $T$  of the map  $\Phi_N$  is the same as the number of MPOs with the period  $N$  of the map  $\Phi_T$ . Equivalently:*

$$(4.1) \quad (-1)^N \det(I - \mathfrak{B}_N^T) = (-1)^T \det(I - \mathfrak{B}_T^N).$$

*Proof:* Straightforwardly follows from Lemma 4.1 and eq. (3.7).  $\square$

Since the spectrum of matrix  $\mathfrak{B}_N$  is known explicitly, eq. (4.1) allows to extract a couple of interesting mathematical identities.



**Corollary 4.4.** *Let  $\cosh \beta_k = s/2 - \cos(2\pi k/N)$ ,  $\cosh \tilde{\beta}_k = s/2 - \cos(2\pi k/T)$ , with  $T, N$  being integers and  $s \geq 4$  then:*

$$(4.2) \quad \prod_{k=1}^N 4 \sinh^2 \left( \frac{T\beta_k}{2} \right) = \prod_{m=1}^T 4 \sinh^2 \left( \frac{N\tilde{\beta}_m}{2} \right).$$

After taking the limit  $s \rightarrow 0$  this equation leads to:

$$(4.3) \quad T^2 \prod_{k=1}^{N-1} 4 \sin^2 \left( \frac{\pi k T}{N} \right) = N^2 \prod_{m=1}^{T-1} 4 \sin^2 \left( \frac{\pi m N}{T} \right).$$

In particular, for  $T = 1$  we obtain the well known identity:

$$\prod_{k=1}^{N-1} \sin \left( \frac{\pi k}{N} \right) = \frac{N}{(-2)^{N-1}}.$$

**4.1. Duality between partner orbits.** The duality relationship has very important implication on the correlation mechanism between periodic orbits of the system. In particular, it implies that pairs of partner orbits of a period  $T$  with the encounter structure given by winding numbers  $(w_1, w_2)$  for the  $N$ -particle system are in one-to-one correspondence with the pairs of partner orbits of the period  $N$  with the encounter structure  $(w_2, w_1)$  for the  $T$ -particle system. For a small number of particles  $N$  and large times  $T$  it is natural to expect that most of the partner orbits poses  $(0, 1)$  type of encounters. The duality relationship shows that the opposite regime when  $T$  is large and  $N$  is small is dominated by the partner orbits with inverse winding numbers  $(0, 1)$ . In a sense these two regimes are dual to each other. For instance, the number of partner orbits and their action differences must coincide. Although the exact duality relationship i.e., Lemma 4.1 holds only under specific condition  $c = d$ , we believe that in its weaker sense, as connection between correlation mechanism in the above regimes it makes sense for general parameters  $a, b, c, d$ .

## 5. MANY PARTICLE PARTNER ORBITS

The main goal of the present section is an explicit construction of partner MPO's with close actions. Here we restrict our attention to the case of the non-perturbed maps  $\Phi_N$  with  $\mathcal{V} = 0$ . A remarkable property of the non-perturbed cat maps is that their periodic orbits traverse the points of the phase space with rational coordinates and can be found exactly rather than as an approximation. Furthermore, their actions are given by rational numbers and can be explicitly evaluated, as well.

**5.1. Symbolic dynamics.** As it was explained in the section (2), a convenient representation of partner MPO's can be achieved by means of 2D symbolic dynamics with a finite alphabet. To introduce the symbolic representation we use as the alphabet the set of winding numbers  $m_{n,t}^p, m_{n,t}^q$  entering the dynamical equations of

motions (3.2). For each moment of time we define the vector

$$\mathbf{m}_{n,t} = \begin{pmatrix} m_{n,t}^q \\ m_{n,t}^p \end{pmatrix}, \quad \mathbf{M}_t = (\mathbf{m}_{1,t} \quad \mathbf{m}_{2,t} \quad \dots \quad \mathbf{m}_{N,t})^T.$$

Note that the whole set of these vectors from  $t = 1$  up to  $t = T$  uniquely defines the corresponding periodic orbits. Indeed, the global winding number vector  $\mathcal{M}_\Gamma$  of a periodic trajectory  $\Gamma$  can be restored from  $\mathcal{M}_t$  by:

$$(5.1) \quad \mathcal{M}_\Gamma = \sum_{t=1}^T \mathfrak{B}_N^{T-t} \mathbf{M}_t.$$

This vector can be used then in order to restore the initial conditions for the MPO:

$$(5.2) \quad Z_0 = (\mathfrak{B}_N^T - I)^{-1} \mathcal{M}_\Gamma.$$

As a result the following matrix of winding numbers,

$$(5.3) \quad \mathbb{M}_\Gamma = \begin{pmatrix} m_{1,1} & m_{2,1} & \dots & m_{N,1} \\ m_{1,2} & m_{2,2} & \dots & m_{N,2} \\ \vdots & \vdots & \ddots & \vdots \\ m_{1,T} & m_{2,T} & \dots & m_{N,T} \end{pmatrix},$$

can be seen as the unique symbolic representation of  $\Gamma$ .

Importantly, because of the local nature of the interactions the integer vectors  $\mathbf{m}_{n,t}$  can take only a finite number of possible values. Accordingly we obtain 2D-symbolic representation of periodic orbits with a small alphabet, whose size is independent of  $N$ .

**5.2. Construction of partner MPOs .** Our construction of partner MPO's with the prescribed encounter structure can be divided into few steps which are described below and schematically summarized in the fig. 8.

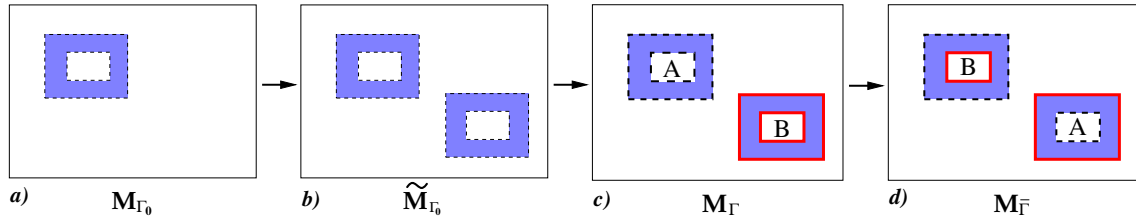


FIGURE 8. 4-Step construction of partner MPOs.

*Step 1 (fig. 8a).* As the first step, we generate a random periodic trajectory  $\Gamma_0$  and its symbolic representation  $\mathbb{M}_{\Gamma_0}$  by means of the following procedure. Let  $\mathcal{M}_0$  be an arbitrary vector of integers. Then the initial conditions for the corresponding MPO can be obtained by

$$(5.4) \quad Z_0 = (\mathfrak{B}_N^T - I)^{-1} \mathcal{M}_0 \mod \mathbf{1},$$

where  $Z_0$  is the  $2N$  dimensional vector of coordinates and momenta at the initial moment of time. The rest part of the orbit is obtained by iterative action of the matrix  $\mathfrak{B}_N$  on the vector  $Z_0$ . Note, that since the entries of the matrix  $\mathfrak{B}_N$  are integers, the coordinates of the MPO are rational numbers. This property of the map allows to calculate the orbits explicitly avoiding any numerical approximation.

*Step 2 (fig. 8b).* Recall that a partner orbit for any MPO  $\Gamma$  might exist only if it has (at least) one encounter. In other words certain pattern of symbols in symbolic representation of  $\Gamma$  must reappear for a number of times. Naturally, for small  $N$  and  $T$  a generic MPO does not satisfy this property and the purpose of this step is to prepare such an orbit. For that we choose some region of a given shape in the original  $\mathbb{M}_{\Gamma_0}$ , which is then copied and pasted into another location of  $\mathbb{M}_{\Gamma_0}$ . The resulting sequence of symbols  $\tilde{\mathbb{M}}_{\Gamma_0}$  has the correct encounter structure, but, in general, does not correspond to any real MPO.

*Step 3 (fig. 8c).* In order to generate 2D sequence corresponding to a valid periodic orbit we now use  $\tilde{\mathbb{M}}_{\Gamma_0}$  as an initial data for eq. (5.1). More specifically, let  $\tilde{\mathbb{M}}_t := \tilde{\mathbb{M}}_{\Gamma_0}(t)$  be the  $t$ -th column of the matrix  $\tilde{\mathbb{M}}_{\Gamma_0}$ . We define the integer vector:

$$(5.5) \quad \tilde{\mathcal{M}}_0 = \sum_{t=1}^T \mathfrak{B}_N^{T-t} \tilde{\mathbb{M}}_t,$$

which is then used as the input for the right hand side of eq. (5.4) in order to generate the corresponding MPO. Denote this periodic orbit as  $\tilde{\Gamma}$  and its 2D symbolic representation as  $\tilde{\mathbb{M}}_{\tilde{\Gamma}}$ . The crucial observation is that  $\mathbb{M}_{\tilde{\Gamma}}$  and  $\tilde{\mathbb{M}}_{\Gamma_0}$  differ only locally at the places of encounter boundaries. As a result, we obtain the MPO  $\tilde{\Gamma}$  with the desired encounter structure.

*Step 4 (fig. 8d).* At this stage we can construct the partner orbit  $\bar{\Gamma}$  of  $\tilde{\Gamma}$  by rearranging the symbols  $\mathbb{M}_{\tilde{\Gamma}}$  outside of the encounter regions, into a new 2D sequence  $\mathbb{M}_{\bar{\Gamma}}$  as has been explained in Section 2. Note that this new sequence of symbols is in general symbolic representation of a real MPO  $\bar{\Gamma}$  which can be straightforwardly recovered from  $\mathbb{M}_{\bar{\Gamma}}$  by eqs. (5.1,5.2). By construction  $\bar{\Gamma}$  and  $\tilde{\Gamma}$  are partner MPO's traversing approximately the same points of the phase space.

**Remark 5.1.** *In principle it might happen that the 2D symbolic sequence obtained from  $\mathbb{M}_{\tilde{\Gamma}}$  by exchange of the sequences A and B (see fig. 8) differs from 2D symbolic sequence  $\mathbb{M}_{\bar{\Gamma}}$  of the partner orbit  $\bar{\Gamma}$  by a small number of symbols. This should happen whenever one of the two points  $\Gamma_{t,n}$ ,  $\bar{\Gamma}_{t',n'}$  closely approaching each other in the phase space turn out to be encoded by two locally different symbolic subsequences. We however have not observed such a phenomena in our numerical constructions of partner MPO. **think again***

**Remark 5.2.** *One can expect that the 2D symbolic sequence obtained from  $\mathbb{M}_{\tilde{\Gamma}}$  by exchange of the sequences A and B (see fig. 8) sometimes differs from the 2D symbolic sequence  $\mathbb{M}_{\bar{\Gamma}}$  of the partner orbit  $\bar{\Gamma}$  by a small number of symbols. It might happen, for instance, if some two points  $\Gamma_{t,n}$  and  $\bar{\Gamma}_{t',n'}$  are closely approaching each other in the phase space, but encoded by two different symbols. In our numerical*

calculations performed for the non-perturbed maps, see Appendix A, we have not found evidence of such phenomena.

**Example.** In the Appendix A we illustrate the above four step procedure by particular calculation of the partner orbits for the case of non-perturbed coupled cat maps.

**5.3. Action differences.** Keeping in mind applications to quantum mechanics it is of great importance to evaluate the action differences  $\Delta S = S_\Gamma - S_{\bar{\Gamma}}$  between partner orbits  $\Gamma, \bar{\Gamma}$ . Indeed, in a semiclassical theory  $\Delta S$  provide the weights with which periodic orbits of a given encounter structure contribute to spectral correlations [6]. It is known that in the case of single-particle chaotic systems the differences between

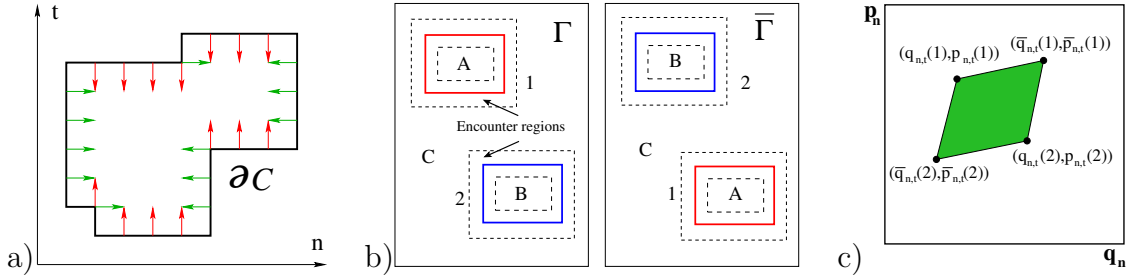


FIGURE 9. The figure (b) in the middle schematically shows two partner MPO together with the encounter domain and a contour inside. On the left figure (a) is shown the magnified caricature of the contour  $\partial C$  where the difference between actions is calculated. The right figure (c) shows the region in the single-particle phase space whose area contributes to eq. (5.10)

actions of partner orbits accumulate at the encounters, where the distance between points is maximal. Below we show that a similar result holds for many particle systems, as well.

By setting in eq. (3.9)  $\mathcal{V} = 0$  we obtain for the total action of  $\Gamma$

$$(5.6) \quad S_\Gamma = \frac{1}{2} \sum_{(n,t) \in \mathbb{Z}_{NT}^2} q_{n,t} m_{n,t}.$$

Let  $\Gamma, \bar{\Gamma}$  be two different MPO such that  $\{q_{n,t}, m_{n,t} | (n,t) \in \mathbb{Z}_{NT}^2\}, \{\bar{q}_{n,t}, \bar{m}_{n,t} | (n,t) \in \mathbb{Z}_{NT}^2\}$  are the corresponding solutions of eq. (3.4). Let us calculate the difference between their actions accumulated in a certain region  $C$  of  $\mathbb{Z}_{NT}^2$ :

$$(5.7) \quad S_\Gamma^{(C)} = \frac{1}{2} \sum_{(n,t) \in C} q_{n,t} m_{n,t}, \quad S_{\bar{\Gamma}}^{(C)} = \frac{1}{2} \sum_{(n,t) \in C} \bar{q}_{n,t} \bar{m}_{n,t}.$$

We will assume that inside of the domain  $C$  the two MPO are close to each other and the corresponding winding numbers coincide i.e.,  $m_{n,t} = \bar{m}_{n,t}$  for  $(n,t) \in C$ . Denote by  $\partial C$  the boundary of  $C$ . Note that if  $C$  is a multiconnected domain then  $\partial C$  is composed of a number of disjoint components. Multiplying both sides of eq. (3.4) for  $\Gamma$  by the coordinates  $\bar{q}_{n,t}$ , and similarly eq. (3.4) for  $\bar{\Gamma}$  by the coordinates  $q_{n,t}$

we obtain two equations containing bilinear forms in  $\bar{q}_{n,t}, q_{n,t}$ . After subtraction of these equations we obtain:

$$(5.8) \quad 2(S_\Gamma^{(C)} - S_{\bar{\Gamma}}^{(C)}) = \sum_{(n,t) \in \partial C_\uparrow} q_{n,t} \bar{q}_{n,t+1} - \bar{q}_{n,t} q_{n,t+1} + \sum_{(n,t) \in \partial C_\downarrow} q_{n,t} \bar{q}_{n,t-1} - \bar{q}_{n,t} q_{n,t-1} \\ + \sum_{(n,t) \in \partial C_\rightarrow} q_{n,t} \bar{q}_{n+1,t} - \bar{q}_{n,t} q_{n+1,t} + \sum_{(n,t) \in \partial C_\leftarrow} q_{n,t} \bar{q}_{n-1,t} - \bar{q}_{n,t} q_{n-1,t},$$

where  $\partial C_\uparrow, \partial C_\downarrow$  and  $\partial C_\rightarrow, \partial C_\leftarrow$  are pieces of the boundary going in the vertical and horizontal directions respectively, see fig. (9a). Note that the points  $(n, t)$  at the corners of the domain  $C$  belong to the both sets simultaneously. Remarkably the right hand side of the above equation contains only the sum over the boundaries of  $C$ .

Let us now evaluate the difference between total actions of  $\Gamma$  and  $\bar{\Gamma}$ . For simplicity of exposition we will assume that there is only one encounter of the order two. In such a case the whole set  $\mathbb{Z}_{\text{NT}}^2$  can be divided into three regions  $A, B, C$  separated by the boundary  $\partial C = \partial A \cup \partial B$  which passes inside of encounter regions, see fig. (9b). Accordingly the action difference can be written as a sum of three terms

$$(5.9) \quad \Delta S = S_\Gamma^{(A)} - S_{\bar{\Gamma}}^{(A)} + S_\Gamma^{(B)} - S_{\bar{\Gamma}}^{(B)} + S_\Gamma^{(C)} - S_{\bar{\Gamma}}^{(C)}.$$

By eq. (5.8) the differences between actions depend only on the boundary values of  $q_{n,t}, \bar{q}_{n,t}$  at  $\partial C$ . As a result the above expression for  $\Delta S$  can be rewritten in a compact form as the sum over the boundary  $\partial C$ :

$$(5.10) \quad \Delta S = \sum_{(n,t) \in \partial C_\parallel} \Delta S_{n,t}^\parallel + \sum_{(n,t) \in \partial C_\perp} \Delta S_{n,t}^\perp,$$

where  $\partial C_\parallel := \partial C_\uparrow \cup \partial C_\downarrow$ ,  $\partial C_\perp := \partial C_\leftarrow \cup \partial C_\rightarrow$  are pieces of the boundary directed in the vertical and horizontal directions respectively. The local action differences are defined here as

$$(5.11) \quad \Delta S_{n,t}^a = [q_{n,t}(2) - q_{n,t}(1)] [\bar{p}_{n,t}^a(2) - \bar{p}_{n,t}^a(1)] \\ + [\bar{q}_{n,t}(2) - \bar{q}_{n,t}(1)] [p_{n,t}^a(2) - p_{n,t}^a(1)], \quad a \in \{\parallel, \perp\},$$

with  $q_{n,t}(k)$  (resp.  $\bar{q}_{n,t}(k)$ ) being the coordinate at the encounter  $k = 1, 2$  of  $\Gamma$  (resp.  $\bar{\Gamma}$ ) and  $p_{n,t}^a(k)$  (resp.  $\bar{p}_{n,t}^a(k)$ ) are the corresponding generalized momenta, see fig. (9b). The relationship of these momenta to the coordinates depends on the direction  $a$  of the boundary at the point  $(n, t)$ :

$$(5.12) \quad p_{n,t}^\parallel(k) := q_{n,t+1}(k) - q_{n,t}(k), \quad p_{n,t}^\perp(k) := q_{n+1,t}(k) - q_{n,t}(k).$$

It worth noticing that the expression (5.11) for  $\Delta S_{n,t}^a$  can be interpreted as a local symplectic area of the region formed by the four points  $(q_{n,t}(k), p_{n,t}^a(k)), (\bar{q}_{n,t}(k), \bar{p}_{n,t}^a(k))$ ,  $k = 1, 2$  in the phase space, see fig. (9c). The representation (5.11) is essentially an extension of the similar result for the single-particle case. There the difference between actions of partner orbits is determined by an analogous symplectic area evaluated at an arbitrary point of their encounter [6].

## 6. SYMMETRIES

So far we have ignored the possibility that the map  $\Phi_N$  might possess a discrete symmetry. Such symmetries are of crucial importance for the associated quantum problem, where they determine which universality class system belongs to. On the classical side of the problem the presence of symmetries gives rise to partner orbits with close actions which do not traverse approximately the same points of phase space, but rather two sets of points related by the symmetry operation. For instance, in the systems with the time reversal invariance there exist also partner orbits which traverse (approximately) the same points of the configuration space but have opposite momenta at some pieces of the trajectories. For this to happen it is sufficient to have just one encounter, which is the case of the original Sieber-Richter pairs [7].

All symmetries of Hamiltonian systems can be divided into two classes. The ones which preserve the form of Hamiltonian's equations are called canonical. For  $2N$  dimensional cat maps they are represented by  $2N \times 2N$  integer matrices  $\mathfrak{C}$ ,  $Z \rightarrow \mathfrak{C}Z$ ,  $Z = (q_1, p_1, q_2, p_2, \dots, q_N, p_N)^\top$  satisfying

$$(6.1) \quad \mathfrak{C}\mathfrak{B}_N\mathfrak{C}^{-1} = \mathfrak{B}_N, \quad \mathfrak{C}^2 = \mathbf{I}.$$

For instance, all maps (3.2) commute with the matrix  $\mathfrak{C} = -\mathbf{I}$  which effects the transformation  $\mathbf{q} \rightarrow -\mathbf{q}$ ,  $\mathbf{p} \rightarrow -\mathbf{p}$ . On the other hand a Hamiltonian system might also have anticanonical symmetries, which reverse the signs of Hamiltonian's equations and the Poisson brackets. The most prominent example of the last one is time reversal symmetry. The anticanonical symmetries of  $\Phi$  are represented by  $2N \times 2N$  integer matrices  $\mathfrak{C}$ , that satisfy

$$(6.2) \quad \mathfrak{C}\mathfrak{B}_N\mathfrak{C}^{-1} = \mathfrak{B}_N^{-1}, \quad \mathfrak{C}^2 = \mathbf{I}, \quad \det \mathfrak{C} = -1.$$

It's easy to check that for  $b = 0$  the map  $\Phi$  has the anticanonical symmetry:

$$\mathfrak{C}(q_1, p_1, q_2, p_2, \dots, q_N, p_N)^\top = (p_1, q_1, p_2, q_2, \dots, p_N, q_N)^\top,$$

which amounts to exchanging of the corresponding moments and coordinates.

Assuming that the map  $\Phi_N$  possesses a symmetry  $\mathbb{S}_{\mathfrak{C}}$  (either canonical or anticanonical) defined by a  $2N \times 2N$  matrix  $\mathfrak{C}$  with integer entries let us describe the structure of partner orbits with one encounter. First observe that each MPO  $\Gamma$  has a pair orbit  $\Gamma^* = \mathbb{S}_{\mathfrak{C}} \cdot \Gamma$  which is obtained by action of the linear map  $\mathfrak{C}$  on the set of points  $\Gamma$ . Both orbits have exactly the same actions. The corresponding partner orbits are obtained then by a recombination of different patches from  $\Gamma$  and  $\Gamma^*$ .

To be more specific consider an orbit  $\Gamma$  having one non-trivial encounter with zero winding numbers  $(0, 0)$ . Such an encounter corresponds to two frame-like regions  $E_1, E_2$  of  $\mathbb{Z}_{\text{NT}}^2$  where 2D symbolic representations of  $\Gamma$  and its conjugate  $\Gamma^*$  are related by the symmetry operation  $\mathbb{S}_{\mathfrak{C}}$  in the following way:

$$(6.3) \quad \mathbb{E} := \psi_\Gamma(E_1) = \psi_{\Gamma^*}(E_2), \quad \mathbb{E}^* := \psi_\Gamma(E_2) = \psi_{\Gamma^*}(E_1).$$

The 2D symbolic representation  $\mathbb{M}_{\bar{\Gamma}}$  of the partner orbit  $\bar{\Gamma}$  is then obtained by copying the interiors  $A, B$  of the encounter regions from  $\mathbb{M}_{\Gamma^*}$  and pasting them into the corresponding places of  $\mathbb{M}_\Gamma$ , as shown in fig. 10. The partner orbit of  $\Gamma^*$

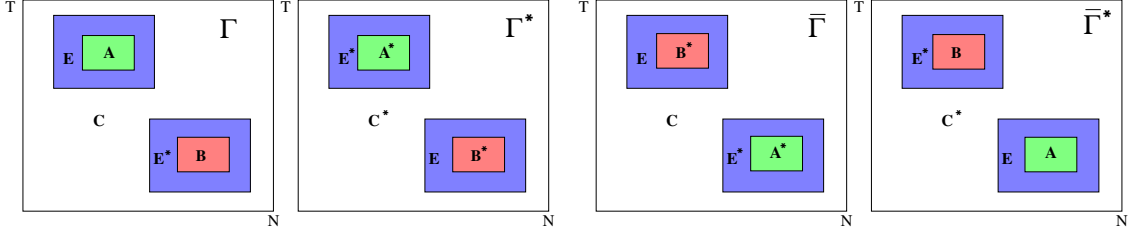


FIGURE 10. On the two left figures are schematically shown the 2D symbolic representations  $\mathbb{M}_\Gamma, \mathbb{M}_{\Gamma^*}$  of some MPO  $\Gamma$  and its symmetric counterpart  $\Gamma^*$  having one encounter with  $(0,0)$  winding numbers. Such conjugate pairs of MPO's with exactly the same action exist whenever the system posses a symmetry. On the two right pictures are depicted the symbolic representations  $\mathbb{M}_{\bar{\Gamma}}, \mathbb{M}_{\bar{\Gamma}^*}$  of the corresponding partner orbits  $\bar{\Gamma}, \bar{\Gamma}^*$ . They are obtained from  $\Gamma$  and  $\Gamma^*$  by copy pasting of the interior regions of encounters. In general  $\bar{\Gamma}, \bar{\Gamma}^*$  (resp.  $\Gamma, \Gamma^*$ ) have close but non-identical actions.

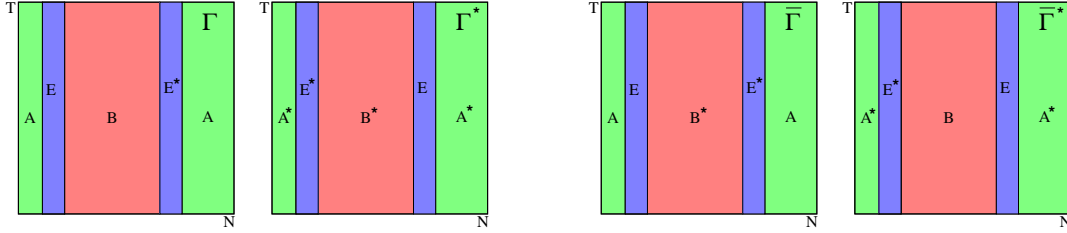


FIGURE 11. On the two left figures are schematically shown the 2D symbolic representations  $\mathbb{M}_\Gamma, \mathbb{M}_{\Gamma^*}$  of symmetrically conjugate MPO's with one encounter having  $(1,0)$  winding numbers. On the two right pictures are depicted the symbolic representations  $\mathbb{M}_{\bar{\Gamma}}, \mathbb{M}_{\bar{\Gamma}^*}$  of the corresponding partner orbits  $\bar{\Gamma}, \bar{\Gamma}^*$ . They are obtained from  $\Gamma$  and  $\Gamma^*$  by copy pasting of the corresponding interior regions of  $\mathbb{M}_\Gamma, \mathbb{M}_{\Gamma^*}$ , as shown in the figure. The partner orbits for MPO's with encounters of the type  $(0,1)$  are constructed in the same way by exchanging particle and time directions.

can readily be obtained by applying symmetry operation to  $\bar{\Gamma}$  i.e.,  $\bar{\Gamma}^* = S_{\mathcal{C}} \cdot \bar{\Gamma}$ . In Appendix B we illustrate the above procedure with an explicit construction of a quadrupole of periodic orbits  $\Gamma, \Gamma^*, \bar{\Gamma}, \bar{\Gamma}^*$ .

For MPO's with one encounter having winding numbers  $(1,0)$  and  $(0,1)$  the construction is analogous. In this case the corresponding encounter regions of  $\mathbb{Z}_{NT}^2$  are two strips winding torus in the particle (resp. time) direction and separating it into two pieces. The symbolic representation of partner orbits is obtained from  $\mathbb{M}_\Gamma, \mathbb{M}_{\Gamma^*}$  by copy pasting of the symbols from these regions, as shown in fig. 11. Note that for the encounters of the type  $(0,1)$  the obtained partner MPO's are the original Sieber-Richter pairs in  $2N$  dimensional phase space of the map  $\Phi_N$ .

## 7. PARTNER MPOs FOR PERTURBED MAP

It is well known that the spectra of quantum cat maps essentially differ from ones of generic chaotic systems [16]. From the semiclassical point of view this anomaly can be attributed to the large degeneracies among the actions of the periodic orbits which are given by rational numbers for a cat map. These degeneracies grow exponentially with the period of orbits [17] leading to the distortion in the distribution of action differences. The genericity, however, may be recovered by adding a periodic nonlinear perturbation [18]. From this prospective it is natural to inquire whether the correlation mechanism between the partner MPOs described in the previous sections carries over to the perturbed coupled cat maps. Below we demonstrate that the answer to this question is indeed affirmative.

Consider the model of perturbed coupled cat maps generated by the function (3.1), where some periodic potential  $\mathcal{V}(q) \equiv \kappa \mathcal{V}_0(q)$  is turned on. We require that,  $\max_q |\mathcal{V}_0''(q)| = 1$  and relate to  $\kappa$  as the strength of the perturbation. The particular choice of the parameter  $\kappa$  is dictated by the requirement that the perturbed map  $\Phi_N$  remains fully chaotic. By the structural stability of classical chaos this is guaranteed for sufficiently small  $\kappa$ . A maximum possible range for  $\kappa$  can be estimated by considering the linearized form of the map  $\Phi_N$ . Let  $q_{n,t}, n = 1, 2, \dots, N$  be some solution of eq. (3.4) and let  $\delta q_{n,t}$  be a small deviation from it. After substituting  $q_{n,t} + \delta q_{n,t}$  into the equations of motion (3.4) and leaving out only linear terms we obtain

$$(7.1) \quad \delta q_{n,t+1} + \delta q_{n,t-1} - d(\delta q_{n+1,t} + \delta q_{n-1,t}) = (s + \mathcal{V}''(q_{n,t}))\delta q_{n,t}.$$

By comparison with the non-perturbed case analysis in Section 3.2 we arrive to the inequality  $|\kappa| < \kappa_{\max} = |s| - 2|d| - 2$ . It can be expected that under this condition the perturbed map  $\Phi_N$  is fully hyperbolic.

**7.1. Construction of MPO partners.** In general, calculating periodic orbits of a non-integrable system is a non-trivial task. To this end a number of methods have been developed, see e.g., [24]. Our approach is based on the minimization of the perturbed action, i.e., the generating function  $S(q_{n,t})$  with respect to  $q_{n,t}$ . The procedure goes as follows. One starts from a MPO  $\Gamma_0 = \{q_{n,t}^{(0)} | (n,t) \in \mathbb{Z}_{\text{NT}}^2\}$  of a non-perturbed map and adds a small perturbation  $\delta\kappa \mathcal{V}_0(q)$  to the action. By structural stability of chaotic dynamics it can be expected that, for a small  $\delta\kappa$  the non-perturbed orbit lays in the vicinity of the perturbed one  $\Gamma_1 = \{q_{n,t}^{(1)} | (n,t) \in \mathbb{Z}_{\text{NT}}^2\}$  which can be easily found by minimization of the action  $S(q_{n,t})$  by using the standard gradient descent method. At the next step one takes  $\{q_{n,t}^{(1)}\}$  as the initial data for the gradient descent method and obtains a new MPO  $\Gamma_2$  for the doubled strength of the perturbation  $2\delta\kappa$ . By iterating this procedure  $m$  times one arrives to a periodic orbit  $\Gamma_m$  which is a smooth deformation of  $\Gamma_0$  for the perturbation of the strength  $\kappa = m\delta\kappa < \kappa_{\max}$ . Importantly, if we start from two partner orbits  $\Gamma_0, \bar{\Gamma}_0$  with the related matrices  $\mathbb{M}_{\Gamma_0}, \mathbb{M}_{\bar{\Gamma}_0}$  of winding numbers, this relationship persists at each step of the iterations. This means that the resulting MPOs  $\Gamma_m, \bar{\Gamma}_m$  are again partners



with small action differences, whose symbolic representations are related in the same way as ones of the initial orbits.

In Appendix C we give an example of explicit calculation of a pair of MPOs  $\Gamma, \bar{\Gamma}$  for the perturbed coupled cat map and demonstrate stability of the pairing phenomena. Namely, we show that all the points of  $\Gamma$  and  $\bar{\Gamma}$  are paired and their action differences accumulate in the encounter regions.

**7.2. Action differences.** It is instructive to see how the formula (5.10) for action differences between the partner orbits is affected by the perturbation. In accordance with eq. (3.9) the actions get extra terms depending on  $\mathcal{V}$ . After repeating the same steps as in the derivation of the non-perturbed case we end up with the additional term in the right hand side of eq. (5.8):

$$\delta S^{(C)} = \sum_{(n,t) \in C} \frac{1}{2} \left( \mathcal{V}'(\bar{q}_{n,t}) + \mathcal{V}'(q_{n,t}) \right) (q_{n,t} - \bar{q}_{n,t}) - \mathcal{V}(q_{n,t}) + \mathcal{V}(\bar{q}_{n,t}).$$

Like the main contribution in eq. (5.8), the term  $\delta S^{(C)}$  is accumulated mainly in the encounter region. It is straightforward to see, however, that  $\delta S^{(C)}$  is proportional to the third order of  $\delta q_{n,t} := q_{n,t} - \bar{q}_{n,t}$ :

$$\delta S^{(C)} = \sum_{(n,t) \in C} \frac{\delta q_{n,t}^3}{12} \mathcal{V}^{(3)} \left( \frac{q_{n,t} + \bar{q}_{n,t}}{2} \right) + \mathcal{O}(\delta q_{n,t}^5),$$

while the principle term  $S_{\Gamma}^{(C)} - S_{\bar{\Gamma}}^{(C)}$  is of the order  $\delta q_{n,t}^2$ . As a result,  $\delta S^{(C)}$  can be dropped out for MPOs with large encounters (where the distances between the partners are small). Since the same conclusion holds for all other terms in eq. (5.9) it follows immediately that the formula (5.10) is still valid in an approximate sense. The larger the size of encounters, the better approximation gives the equation (5.10).

## 8. CONCLUSIONS

**8.1. Quantum problem.** So far we have studied clustering of MPOs in the context of purely classical theory. While leaving applications to quantum mechanics for future investigations, let us briefly discuss the implications of our results for a semiclassical theory of many-particle systems. Spectral correlations in quantum systems with fully chaotic classical dynamics can be related to correlations between periodic orbits. Consider as an example the spectral form factor  $K_2$  which is defined as the Fourier transform of the two-point spectral correlation function. Via the trace formula it can be expressed as a double sum over pairs of partner periodic orbits. These pairs  $\Gamma, \bar{\Gamma}$  can be clustered in accordance to their topological structures  $\mathcal{F}_{\Gamma}$ , such that:

$$(8.1) \quad K_2(T, N) = \text{Re} \sum_{\mathcal{F}} \sum_{\{\bar{\Gamma}, \Gamma | \mathcal{F}_{\Gamma} = \mathcal{F}\}} \mathcal{A}_{\Gamma} \exp(i\Delta S_{\Gamma}/\hbar_{eff}),$$

where the first sum runs over all possible topological structures  $\mathcal{F}$  of MPOs [6, 25]. The factors  $\mathcal{A}_{\Gamma}$ ,  $\Delta S_{\Gamma}$  are determined by stabilities and by differences between actions

of partner orbits, respectively, with  $\hbar_{eff}^{-1}$  being the integer Hilbert space dimension of the corresponding quantum cat map, see [16].

In order to clarify which topological structures of MPOs are of a relevance for given number of particles  $N$  and time  $T$ , it is of crucial importance to estimate how many periodic orbits  $\Gamma$  posses a given topological structure  $\mathcal{F}$ . The amount of such orbits is determined by the number of possibilities to choose the encounter sets  $E_n^{(k)}, k = 1, \dots, l_n$  within the prescribed topological order. As we argue below this, in turn, depends on the winding numbers  $w_n$  of  $E_n^{(k)}$ 's and their widths  $p_n$ . Note that systematic contribution into the sum (8.1) comes from the terms for which  $\Delta S_\Gamma$  is of the same order as  $\hbar_{eff}$ . This fixes the scale of encounter width as  $p_n \sim |\log \hbar_{eff}|$ . Consider now an encounter set having the winding numbers  $w = (0, 1)$ , i.e., winding around the torus in the particle direction. Such a set occupies at least  $N \cdot p$  points of  $\mathbb{Z}_{NT}^2$ . Analogously, for encounters with winding numbers  $w = (1, 0)$ ,  $w = (0, 0)$  the minimal number of points is given by  $T \cdot p$  and  $p^2$ , respectively. It is easy to see that the number of periodic orbits with the fixed symbols at the encounter domains  $E_n^{(k)}, k = 1, \dots, l_n$  grows exponentially with the total number of points of  $\mathbb{Z}_{NT}^2$  outside of the encounter sets. From this we can immediately conclude that for  $N \ll |\log \hbar_{eff}| \ll T$  most of the periodic orbits have encounters of the type  $w = (0, 1)$ , since they occupy the minimal “area” of  $\mathbb{Z}_{NT}^2$ . For such parameters  $N, T$  the correlations between actions of MPOs can be understood just by interpreting the system dynamics as single-particle motion in many-dimensional phase space. In other words in this regime the semiclassical theory of many-particle systems should be the same as for single-particle systems with chaotic dynamics. In the regime  $T \ll |\log \hbar_{eff}| \ll N$  the dominating encounter type of periodic orbits is  $w = (1, 0)$  and the clustering mechanism is dual to the previous one. This means that correlations between actions of periodic orbits can be accounted by utilizing single-particle theory with the parameters  $N$  and  $T$  exchanged. Finally in the case when both parameters are “large”:  $T, N \gg |\log \hbar_{eff}|$  most of the periodic orbits posses encounters with zero winding numbers  $w = (0, 0)$ . In this case the correlations between actions of MPOs cannot be accounted on the basis of single-particle interpretation of the system dynamics. For this regime a new genuine many-particle semiclassical theory has to be constructed.

**8.2. Generalizations.** The theory proposed in this paper has been constructed and verified in the framework of a specific model of coupled lattice maps. One might wonder whether it carries over to the Hamiltonian systems with continues time evolution. We believe that the main results hold also for generic Hamiltonians of the form (2.1) provided that the dynamics are chaotic. In order to clarify this point consider, as an example, a many-particle periodic orbit  $\Gamma(t) = \{(x_n(t), p_n(t))\}$  where  $t \in [0, T]$  now continues time and the coordinates  $x_n(t)$  satisfy the system of  $N$  Newtonian equations generated by the Hamiltonian (2.1). Assume that  $\Gamma(t)$  has an encounter domain with the frame-like structure shown in fig. 7. In the coordinate form this means that for  $(n, t) \in E$  we have an approximate equality  $x_n(t) \approx x_{n+n'}(t + t')$ , where  $(n + n', t + t') \in E'$  are the points of the shifted encounter set. (For sufficiently large  $T$  and  $N$  such encounters should exist just by

statistical reasons.) Let us now construct another trajectory following the rules for search of partner orbits. To this end define:

$$\bar{x}_n(t) := \begin{cases} x_n(t) & \text{if } (n, t) \notin B \cup A, \\ x_{n+n'}(t+t') & \text{if } (n, t) \in B, \\ x_{n-n'}(t-t') & \text{if } (n, t) \in A. \end{cases}$$

It is now a straightforward observation following from the locality of the Hamiltonian interactions that the set of trajectories  $\bar{\Gamma}(t) = \{(\bar{x}_n(t), \bar{p}_n(t))\}$  approximately satisfies the equations of motion. It follows then from the shadowing lemma for flows of chaotic systems [13] that a real periodic orbit close to  $\bar{\Gamma}(t)$  should exist. By construction this new orbit is the partner of  $\Gamma(t)$ .

Taking a step further one can also question whether discretization in the particle direction might be left out as well. Making  $n$  continues naturally leads to a field model, where the field  $\phi(x, t)$  satisfies some homogeneous differential equation and the continues parameter  $x \in [0, L]$  plays the role of  $n$ . Assuming that the resulting dynamics are chaotic it can be expected that periodic solutions  $\phi_{per}(x, t)$  of the differential equation posses similar properties as MPOs in the coupled lattice maps. In particular we expect that the mechanism of correlations between MPOs carries over to  $\phi_{per}(x, t)$ . We believe that this correlation mechanism can be of importance for development of the semiclassical approach to the corresponding Quantum Field Theory.

Another natural extension of the present setup arises if the particles are ordered with respect to the  $d$ -dimensional lattice i.e.,  $n \in \mathbb{Z}^d$ ,  $d > 1$  rather than to the one-dimensional  $\mathbb{Z}$ . In this case propagating MPOs sweep  $d + 1$ -dimensional “surfaces” in the one-particle phase space. It would be of interest to study how the dimension  $d$  affects the correlation mechanism between MPOs.

**8.3. Summary.** Periodic orbits of chaotic systems can be organized into clusters of partner orbits where all elements have approximately the same actions. The clustering phenomena plays a crucial role for the semiclassical theory. So far however, it has been studied only on the level of effectively “single-particle” systems. In the present work we considered clustering mechanism among periodic orbits of fully chaotic many-particle systems which dynamics are governed by translation-invariant Hamiltonians with local interactions. On the heuristic level periodic orbits in such systems can be visualized by discretized two-dimensional “surfaces” in the one-particle configuration space. A more rigorous description is achieved by using symbolic dynamics. Contrary to the single-particle formalism, where periodic orbits are encoded by linear symbolic sequences, here the symbolic representation is provided by 2D toric arrays of symbols. A periodic orbit  $\Gamma$  has a partner  $\bar{\Gamma}$  when its symbolic representation  $\mathbb{A}_\Gamma$  has at least one  $l$ -encounter - a 2D subsequence of symbols repeating itself for  $l > 1$  of times. The symbolic representations  $\mathbb{A}_{\bar{\Gamma}}$  of the partner orbits are then obtained by rearrangement of symbols  $\mathbb{A}_\Gamma$  in accordance to certain prescription. The differences between actions of  $\Gamma$  and its partners accumulate mainly in the encounter regions and decrease exponentially with their width.

Different families of partner orbits can be distinguished by the corresponding topological structure diagrams. Each structure is represented by a toroidal surface glued to itself along a number of one-dimensional lines representing the encounters. The diagrams with encounters winding around torus only in the particle direction are the ones which obtained in the single-particle interpretation of classical dynamics. The other structural diagrams are essentially different. They represent partner periodic orbits whose correlation mechanism differs from one found in single-particle systems. These new families of partner orbits seem to be essential for construction of a proper semiclassical theory in the case when the number of particles is sufficiently large.

#### ACKNOWLEDGMENTS:

We are grateful to M. Akila, P. Braun, T. Guhr and D. Waltner for useful discussions. Financial support by SFB/TR12 and DFG research grant Gu 1208/1-1 is gratefully acknowledged.

#### REFERENCES

- [1] P. Cvitanović, R. Artuso, R. Mainieri, G. Tanner and G. Vattay, *Chaos: Classical and Quantum*, [ChaosBook.org](http://ChaosBook.org) (Niels Bohr Institute, Copenhagen 2012)
- [2] O. Bohigas, M. J. Giannoni and C. Schmit, *Phys.Rev.Lett.* **52**, 1 (1984)
- [3] M. Berry, *Proc. R. Soc. A* **400**, 229(1985)
- [4] N. Argaman, F.M. Dittes, E. Doron, J.P. Keating, A. Kitaev, M Sieber, U. Smilansky *Phys. Rev. Lett.* **71**, 4326 (1993)
- [5] D. Cohen, H. Primack, U. Smilansky *Ann. Phys.* **264** 108 (1998)
- [6] F. Haake, *Quantum Signatures of Chaos*, 3rd ed. (Berlin: Springer-Verlag, 2010)
- [7] M. Sieber and K. Richter, *Phys. Scripta.* **T90**, 128 (2001)
- [8] M. Sieber, *J. Phys. A* **35** L613 (2002)
- [9] S. Müller, S. Heusler, P. Braun, F. Haake and A. Altland, *Phys. Rev. Lett.* **93**, 014103 (2004); *Phys. Rev. E* **72**, 046207 (2005)
- [10] T. Engl, J. Dujardin, A.Argüelles, P.Schlagheck, K.Richter, J.D.Urbina, *Phys.Rev.Lett.* **112**, 140403 (2014)
- [11] J.D. Urbina, J.Kuipers, Q.Hummel, K.Richter *arXiv:1409.1558v1*
- [12] V.I. Arnold, *Mathematical Methods of Classical Mechanics*, ( Springer-Verlag, 1989)
- [13] A. Katok, B. Hasselblatt, *Introduction to the Modern Theory of Dynamical Systems* (Cambridge University Press,1995)
- [14] B. Gutkin, V.Al. Osipov, *Nonlinearity* **26** 177 (2013)
- [15] B. Gutkin, V.Al. Osipov, *J. Stat. Phys.* **153**, 1049 (2013)
- [16] J.P Keating (1991), *Nonlinearity* **4**, 309-341
- [17] J.P. Keating, *Nonlinearity* **4**, 277 (1991)
- [18] P.A. Boasman J.P. Keating , *Proc. R. Soc. Lond. A* **449**, 629 (1995)
- [19] A.M.F. Rivas, M. Saraceno, A.M.O. de Almeida *Nonlinearity* **13**, 341 (2000)
- [20] J.H. Hannay, M.V. Berry, *Physica 1D*, 267 (1980)
- [21] K. Kaneko, *Formation, Dynamics, and Statistics of Patterns*, edited by K. Kawasaki, et. al. (World Scientific, Singapore 1990)
- [22] S.D. Pethel, N.J. Corron, E. Boltt, *Phys.Rev.Lett.* **99**, 214101, (2007)
- [23] Symbolic dynamics of coupled map lattices S.D. Pethel, N.J. Corron, E. Boltt, *Phys.Rev.Lett.* **96**, 34105 (2006)
- [24] M.Baranger, K.T.R.Davies, J.H.Mahoney, *Annals of physics* **186** (1988) 95
- [25] D.Waltner *Semiclassical approach to mesoscopic systems*, Springer, Berlin (2012)

C315D42045E8D314E360306B100311232002C6013B05B5056C00403035A06B33005C45  
 2316C3253B21C71B533005B2A52C32B3106B8B5240012033B053B503333B2C6C8B54  
 C60B03B830323C5B313C1E10B6C113B501A33B30503300B5102B06B135C610403320  
 C322035E32C31B3133005B8A501053C50263B2C03103A031032006C5E05205053B8  
 3B130053B30026C6E502B1504C6E6B030343B233226C31021C50B51B51133B3A30A3  
 3014E53B130305B61013302054C51015B04C6B1026C00133C33C3C631051C6B5106021  
 32A15B7C22A5010025B3A330320505302B052AB0D30007E0B6230306C015B2303B  
 3B3515B50330035E3D4B4B741B9B35C5E60006B5307E0B4153C10330A8B101A  
 B316016B0136C045B100001502322027D6050525B51A13522C0320323301B6C3306  
 C6C6F620501150315A0550B16E426C6B3C613B4B233C5C6B13311034B305C0153326  
 C6D45115B5A5320352A3400115026B55C8B5032B032532B5A0521B6B2304005B8B003  
 06C630512301B8A350C50253060C3E35A01B6C501B30305A06P510B4E6C0750221  
 06B30C1330522B5C36A1321B3C32B5511330C62133313106321003521043B30B4403  
 023335C043B05A16B9B8B4B2C8B130B6B061B2B4B3E6B4B150102B11B8C6C222D6020  
 C601B7A6030203B32AB804005B0B22B230223A131C6C306C305522012300B01B02  
 032A303013330B1221C326B8A0520B314B1A06C1F8B31311B43220502B0C5506  
 23B1B35000130C35C6C30260F6B05B3B410035B03E6B30305A8C6B01B632E53B6E  
 13352ABBA0300033C6B30306C015B5B503B52B4A531B703039A103030B030240060  
 006B6C00C6B307H1B3B313C10330A8C42C303130500B65B6B6B3C12A5C303053212  
 2030525B51A13522C0320323301106B8B1220303032035B10B31514B3B310  
 3213B4B233C5C6B13311034B305D25A4A042111B52B06B35AB3125D301136B205C  
 B32B32B2032532B5A0521B6B23040012200B3AA053B5203A11524B11C62D0B6302062  
 30135C501B30305A06D510B4E6C07E630E00040A3031076B56205B0B320323B  
 33B1532133313106321003521043B30B123302C0B31A0324C45B3B25C05A3040  
 1B2B3B4B3E6B4B150102B11B8C6C222B3B4C52C8C15C330303B35013B5305C0325C3  
 0061B3A131C6C306C305522012300B05C3B3035C35C102A050100005B3042031B35  
 2A3B1A606C1F8B31311B43220502B0C503122B21A34235C610505C3211B6B6B301  
 031110035B03E6B0305A8C6B01B63A3B061B31133030303B303C6B305C1E6B5B8C2A  
 C6C6A52B4A53100333A33B3030B031501033015B43C1250B5304C60305B33F623C  
 B25003133050300300306B3A12A5C30C15C3B10A53C8C35061223C2B5B53C43106B35  
 B6B8B122303030020C303B10331512B8405B061A123B6B20413B612105B8A4423B  
 3C532111B52B06B35AB3125D301136B0126030C6001405B2603B5B0610622B2A260B6  
 104B5AA053B5203A11524B11C62D0B630206C305B1053C421B00B6C605A3B103B652B  
 5A5B00040A3031076B56205B0B320323B5A3030022B33B25A332000B140B2B23B5  
 E6B3302C0B31A0324C45B3B25C0C43013B403303503315C133A02B2503326  
 00552C8C15C330303B35013B5305C516C33203B323010B6B50B603305B3B3A3033  
 5510B3035C35C102A050100005B3042033A0430320433C50101221311106205E6104B  
 B603021A34235C610505C3211B6B616C3031103B46C720052025F6220B50140C5  
 2003113030330303B303C6B305C1E6B5B8B313C505A3A3C8A1101B5B3003122C5001  
 E5233015B043C1250B5304C60305B33A506A6B6B3030421A5B6303403034B0301326  
 041B10A530C630561223C2B5B5304203310B31C323B303B501B6332002C50000133B13  
 A35102061A123B6B30413B612105B8405B061112301B62B07113B6B30300235C53  
 A13230C6001405B2603B5B0610622B233B1C830205A30A24A6C5C325E61A341B2B3  
 B4B0305B10530421B00B6C63C51B6B501B335E06B321C51B35B2306C12153B3230A  
 205C3022B23225A332000B140B2B23B5106B1233A314C31353B25B6B032C30505C32  
 C64042010503031C0400202C01B23006B2B413500B2B3B103B5103B6B6C6A5C63  
 21B35C6B8B5C031B5303C6C310361C5C7013303B052B303C525F53020502013B6A03  
 C8A1104050042050B8105E623C6C0130050A20B64501126C60B104E5330313203B011  
 5B6C30301501104E5B500C53C0C3B8B005B5E225F6A305B301114E5B500C5B5E2  
 3233B6B8A5E9C052212121624B3132B30062C7C3533C701B130305320535A232125C

FIGURE 12. Symbolic representations  $\mathbb{A}_\Gamma$  (left)  $\mathbb{A}_{\bar{\Gamma}}$  (right) of the two partner periodic orbits  $(\Gamma, \bar{\Gamma})$  for parameters  $a = 3, b = 2, c = d = -1, T = 50, N = 70$ . The corresponding elements of the matrices  $\mathbb{M}_\Gamma$  and  $\mathbb{M}_{\bar{\Gamma}}$  are encoded by the hexadecimal numbers in accordance with the table (8.2). The identical encounter regions are highlighted by green (color on-line). The coinciding inner regions of the encounters (which are exchanged in  $\Gamma$  and  $\bar{\Gamma}$ ) are colored by the identical colors (blue and dark blue).

## APPENDIX A

In this section we construct explicit example of two partner MPOs for the map  $\Phi_N$  with the parameters:  $N = 70, a = 3, b = 2, c = d = -1$ . The initial vector  $\mathcal{M}_0$  in the equation (5.4) is generated as a set of random integers taken from the interval  $[-10^{21}, 10^{21}]$ . The two partner MPOs of the period  $T = 50$  were generated following the protocol described in Section 5.2, see also the explanatory scheme on the figure (8). The resulting symbolic representations  $\mathbb{A}_\Gamma, \mathbb{A}_{\bar{\Gamma}}$  are presented on the picture 12, where each of 16 valid pairs of winding numbers  $m = (m^{(q)}, m^{(p)})$  (see figure 12) is encoded by a symbol  $a$  from the hexadecimal alphabet  $\mathcal{A}$ . The correspondence between symbols of  $\mathcal{A}$  and winding numbers is provided by the table below:

$$(8.2) \quad \begin{array}{c|cccccccccccccccc} m & \begin{pmatrix} 0 \\ 0 \end{pmatrix} & \begin{pmatrix} 0 \\ 1 \end{pmatrix} & \begin{pmatrix} 1 \\ 1 \end{pmatrix} & \begin{pmatrix} 1 \\ 2 \end{pmatrix} & \begin{pmatrix} 1 \\ 3 \end{pmatrix} & \begin{pmatrix} 2 \\ 3 \end{pmatrix} & \begin{pmatrix} 2 \\ 4 \end{pmatrix} & \begin{pmatrix} 2 \\ 5 \end{pmatrix} & \begin{pmatrix} 3 \\ 5 \end{pmatrix} & \begin{pmatrix} 3 \\ 6 \end{pmatrix} & \begin{pmatrix} 0 \\ -1 \end{pmatrix} & \begin{pmatrix} -1 \\ -1 \end{pmatrix} & \begin{pmatrix} -1 \\ -2 \end{pmatrix} & \begin{pmatrix} -2 \\ -3 \end{pmatrix} & \begin{pmatrix} -2 \\ -4 \end{pmatrix} \\ \hline a & 0 & 1 & 2 & 3 & 4 & 5 & 6 & 7 & 8 & 9 & A & B & C & D & E & F \end{array}$$

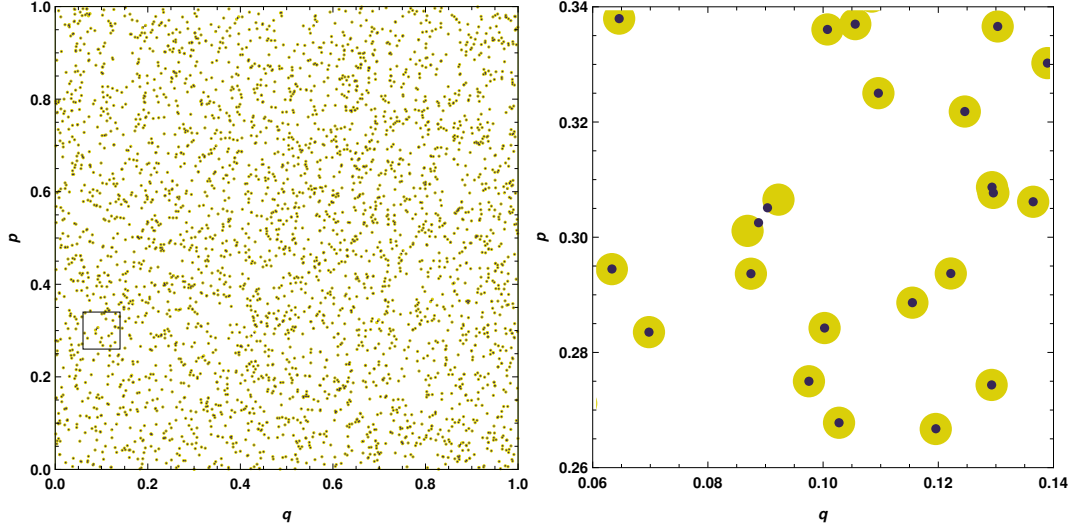


FIGURE 13. *Left:* The phase-space coordinates of the pair of MPOs  $\Gamma, \bar{\Gamma}$  encoded by the symbolic 2D sequences  $\mathbb{A}_\Gamma, \mathbb{A}_{\bar{\Gamma}}$  on the fig. 12. The positions of particles belonging to  $\Gamma$  are depicted by the green circles, while the positions of particles of the orbit  $\bar{\Gamma}$  are the blue circles of smaller sizes. All green and blue points come in pairs and there are no unpaired points. *Right:* The enlarged region of the phase space (the selected rectangle on the left picture). The geometrical centers of the circles visually coincide for almost all points except the four points in the middle of the diagram.

On the fig. 12 the encounter regions of the orbits  $\mathbb{A}_\Gamma, \mathbb{A}_{\bar{\Gamma}}$  are colored in green. One can easily verify that the symbolic sequences inside these regions coincide with each other. Note that the shape of the green areas slightly differs on its borders from the rectangular shape (colored in yellow) of the original encounter-patches. As it is clearly seen, the deformation on the border of legitimate fields causes only local transformation in the symbolic representation.

To evaluate the actual distances between the partner orbits in the phase space we have restored their coordinates and momenta  $\Gamma = \{(q_{n,t}, p_{n,t}) | (n, t) \in \mathbb{Z}_{\text{NT}}^2\}$ ,  $\bar{\Gamma} = \{(\bar{q}_{n,t}, \bar{p}_{n,t}) | (n, t) \in \mathbb{Z}_{\text{NT}}^2\}$  from the corresponding matrices of winding numbers  $\mathbb{M}_\Gamma, \mathbb{M}_{\bar{\Gamma}}$ . The resulting sets of the points in the phase space  $V$  are shown on fig. 13 by the black points for  $\Gamma$  and by the green circles for its partner  $\bar{\Gamma}$ . As one can immediately see, all the points of two orbits are coupled into pairs separated by very small distances. For some points the distances are somewhat larger and the pairs form quadruples, see the enlarged region of the phase space on the fig. 13. These special points correspond to the encounter region of the orbits.

To quantify the metric distances between partner orbits we have calculated the mean square displacement in the phase space for each couple of the paired points. The value of the displacement  $d_{n,t}$  for the particle number  $n$  at time  $t$  is given by

$$(8.3) \quad d_{n,t} = \sqrt{(q_{n,t} - \bar{q}_{n',t'})^2 + (p_{n,t} - \bar{p}_{n',t'})^2},$$

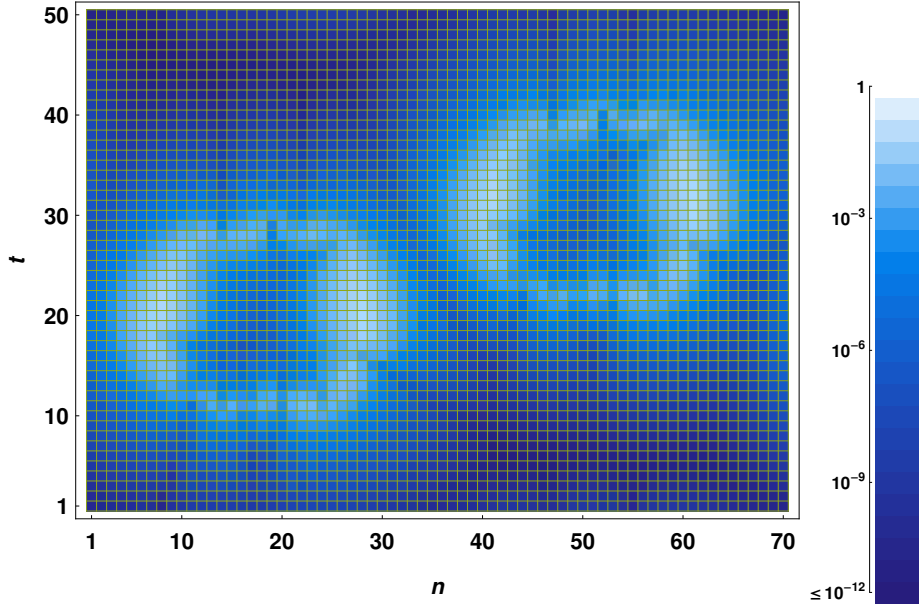


FIGURE 14. Diagram of metric distances between MPOs  $\Gamma$  and  $\bar{\Gamma}$  from the fig. 12. The distances are calculated according to the formula (8.3). The maximal distance between points is  $\simeq 1.7889 \times 10^{-3}$ . The numeric error is of the order  $\simeq 10^{-14}$ .

where  $(\bar{q}_{n',t'}, \bar{p}_{n',t'}) \in \bar{\Gamma}$  is the point paired to the one  $(q_{n,t}, p_{n,t}) \in \Gamma$ . The diagram of the metric distances is plotted on the figure 14. As expected, the largest distances  $d_{n,t} \sim 10^{-3}$  are observed in the encounter regions (appearing as white areas on the figure 12). Outside of the encounters the separations between partner orbits are extremely small with  $d_{n,t} \lesssim 10^{-12}$ .

## APPENDIX B

In this appendix we explicitly construct the quadruple of orbits  $\Gamma$ ,  $\Gamma^*$ ,  $\bar{\Gamma}$ ,  $\bar{\Gamma}^*$  of the period  $T = 50$  for the same map  $\Phi_N$  as in Appendix A. As has been explained in Section 6 this map possesses the symmetry  $\mathbb{S}_{\mathcal{C}}$ :  $\mathbf{q} \rightarrow 1 - \mathbf{q} \bmod 1$ ,  $\mathbf{p} \rightarrow 1 - \mathbf{p} \bmod 1$ . To construct partner orbits which traverse different points of the phase space  $V$  we utilize 4-step protocol similar to one used in Appendix A. First, we generate a random MPO  $\Gamma_0$ , its symmetric counterpart  $\Gamma_0^*$  and the corresponding matrices of winding numbers  $\mathbb{M}_{\Gamma_0}$ ,  $\mathbb{M}_{\Gamma_0^*}$ . We then take a frame-like region  $E_1 \subset \mathbb{Z}_{\text{NT}}^2$  and superimpose the local winding numbers of  $\mathbb{M}_{\Gamma_0^*}$  at  $E_1$  upon another (shifted) region  $E_2 \subset \mathbb{Z}_{\text{NT}}^2$  of  $\mathbb{M}_{\Gamma_0}$ . The resulting matrix  $\tilde{\mathbb{M}}_{\Gamma_0}$  has two regions  $E_1$ ,  $E_2$  satisfying (6.3). Note, however, that  $\tilde{\mathbb{M}}_{\Gamma_0}$  does not correspond to any real MPO. In order to obtain matrix of winding numbers for a valid periodic orbit we then apply eq. (5.5) (see step 3 in Section 5.2). This yields to the matrix  $\mathbb{M}_{\Gamma}$  of winding numbers for a valid trajectory  $\Gamma$  with the correct encounter structure. Its symmetric counterpart is obtained by application of the symmetry operation  $\mathbb{S}_{\mathcal{C}}$ . Finally the partner orbits  $\bar{\Gamma}$ ,  $\bar{\Gamma}^*$  are obtained by rearrangement of symbols from  $\mathbb{M}_{\Gamma}$ ,  $\mathbb{M}_{\Gamma^*}$  as shown in fig. 10.



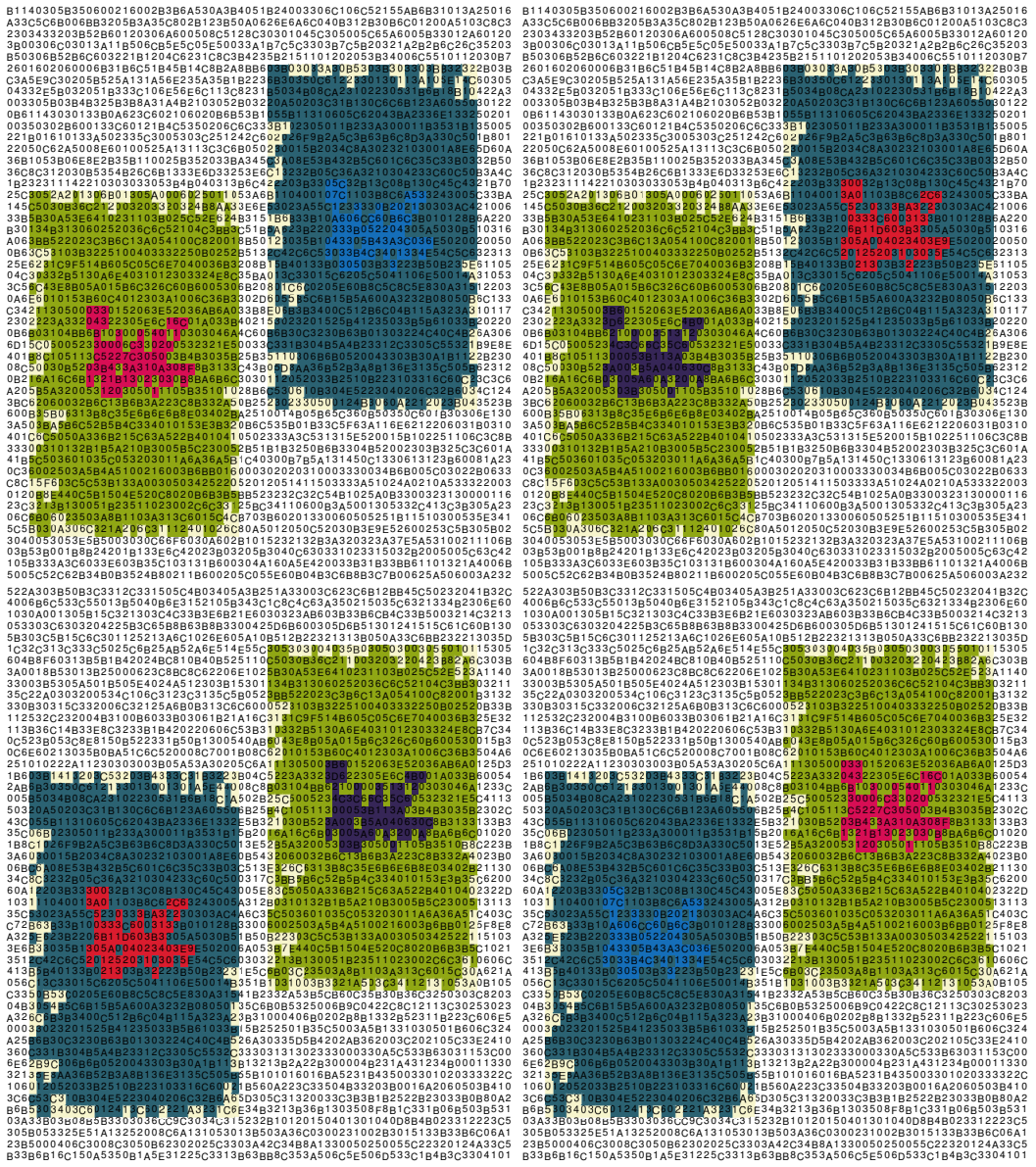


FIGURE 15. Symbolic representations of orbits  $\Gamma_\Gamma$  (upper left)  $\Gamma_{\bar{\Gamma}}$  (upper right)  $\Gamma_{\Gamma^*}$  (down left)  $\Gamma_{\bar{\Gamma}^*}$  (down right) of two partner periodic orbits  $(\Gamma, \bar{\Gamma})$  and their symmetrically conjugate counterparts  $(\Gamma^* = \mathbb{S}_\mathbb{C} \cdot \Gamma, \bar{\Gamma}^* = \mathbb{S}_\mathbb{C} \cdot \bar{\Gamma})$  for  $T = 50$ ,  $N = 70$ . The identical regions of symbols are highlighted by the same color (color on line). The two encounter regions (green and dark-blue) are pairwise conjugated by the symmetry operation  $\mathbb{S}_\mathbb{C}$ .

The resulting symbolic representations of orbits  $\Gamma$ ,  $\Gamma^*$ ,  $\bar{\Gamma}$ ,  $\bar{\Gamma}^*$  are shown in fig. 15. The elements of the matrices  $\mathbb{M}_\Gamma$  (resp.)  $\mathbb{M}_{\bar{\Gamma}}$  are encoded here by the hexadecimal numbers in accordance with the table (8.2). In order to see that  $\Gamma$ ,  $\Gamma^*$ ,  $\bar{\Gamma}$ ,  $\bar{\Gamma}^*$  are indeed partner orbits we plotted on the figure (16) the corresponding sets of



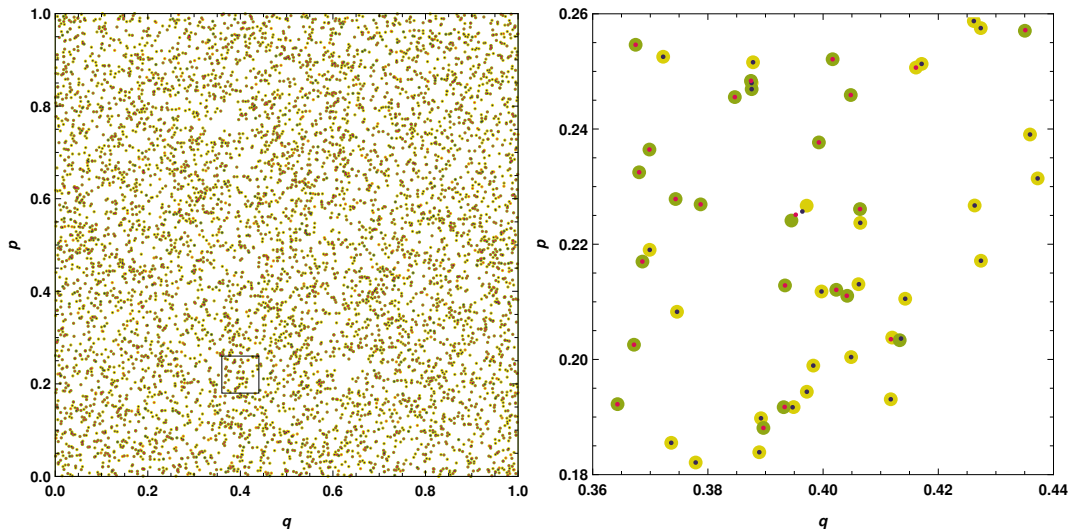


FIGURE 16. *Left:* The phase-space coordinates of the quadruple of orbits  $\Gamma$ ,  $\Gamma^*$ ,  $\bar{\Gamma}$ ,  $\bar{\Gamma}^*$ . The positions of the particles of the trajectories  $\Gamma$  ( $\Gamma^*$ ) are depicted by the large dark (light) green circles. The phase space coordinates of the partner MPOs  $\bar{\Gamma}$  ( $\bar{\Gamma}^*$ ) are depicted by blue (red) circles respectively. All points come in pairs and there are no unpaired points. *Right:* The enlarged region of the phase space (the selected rectangle on the left picture). The geometrical centers of the circles visually coincide for almost all points except the four points in the middle of the plot. These points belong to the encounter region, where the distances between partner orbits are maximal.

momenta and coordinates. It is clearly visible on this plot that any point from  $\bar{\Gamma}$  (resp.  $\bar{\Gamma}^*$ ) closely approaches one of the points from either  $\Gamma$  or  $\Gamma^*$ . In other words all the points of  $\bar{\Gamma}$  and  $\Gamma$  are paired up to the symmetry operation  $S_{\mathcal{C}}$ . As expected, the largest distances between the pairs of the points are observed in the encounters.

## APPENDIX C

In this appendix we present explicit calculations of partner MPOs for the perturbed map. The periodic potential  $\mathcal{V}(q)$  is chosen in the form

$$\mathcal{V}(q) = -\frac{\kappa}{4\pi^2} \cos(2\pi q),$$

with the other parameters of the map set to the same values as in Appendix A. For the sake of convenience we require that the alphabet of the symbolic representation (e.g., the number of symbols) would not change under the perturbation. This can be achieved by a proper choice of the perturbation strength, which in our calculations was set to  $\kappa = 1$ . As we found in our numerical study for this choice of  $\kappa$  the dynamics of the system are chaotic and the symbolic alphabet is still preserved.

The initial partner MPOs  $\Gamma_0$ ,  $\bar{\Gamma}_0$  of the non-perturbed map were taken from our calculations in Appendix A. The partner orbits  $\Gamma$ ,  $\bar{\Gamma}$  for the perturbed map were then constructed following the recipe in Section 7. The two obtained sets of points are

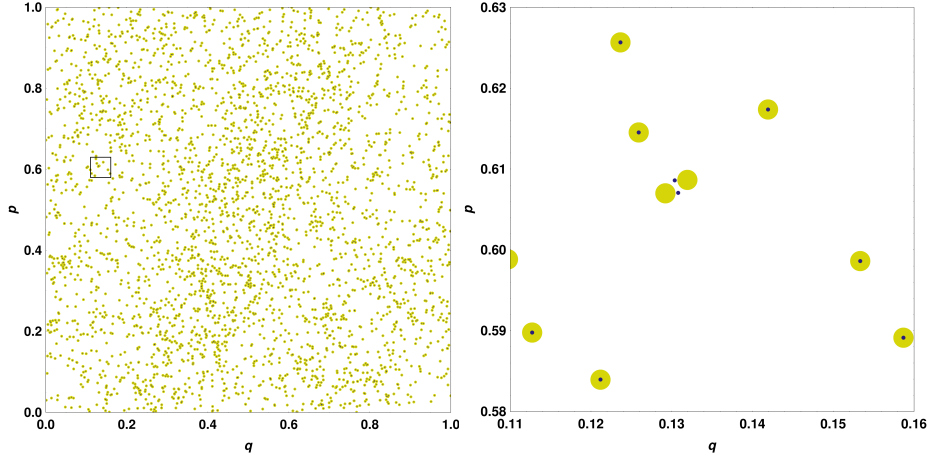


FIGURE 17. *Left*: The phase-space diagram of the pair of MPOs in the case of perturbed map. The coordinates of the orbit and its pair are depicted by the green circles and by the blue circles of smaller size, respectively. All green and blue points come in pairs and there are no unpaired points. *Right*: The enlarged region of the phase space (rectangle on the left picture). The geometrical centers of the circles visually coincide for almost all points except for the four points in the middle of the diagram belonging to the encounter.

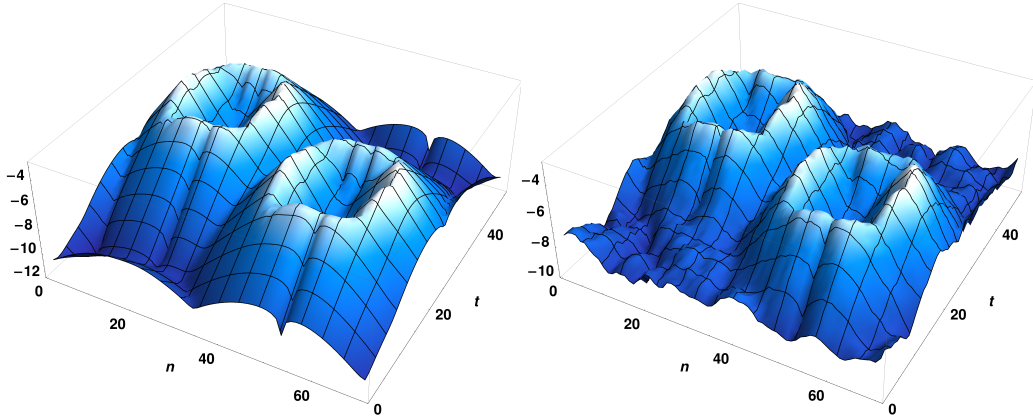


FIGURE 18. 3D diagrams of metric distances for non-perturbed map (left) (2D version of this figure is shown on the fig. 14) and for the perturbed map (right). The maximal distance in the case of the perturbed map is  $\simeq 1.90578 \times 10^{-3}$ , the numeric precision is of the order  $\simeq 10^{-10}$ .

depicted on the fig. 17. As one can see, all the points of partner orbits are coupled into pairs separated by very small distances. In the encounters the distances become larger and the points form quadrupole, see the enlarged region of the phase space on the fig. 17. The metric distances between  $\Gamma$ ,  $\bar{\Gamma}$  were evaluated using the same method as in Appendix A. The result is presented on the fig. 18 in 3D form. For a comparison, the result for the original non-perturbed MPO's  $\Gamma_0$ ,  $\bar{\Gamma}_0$  is shown on the same figure. Although the points of the initial  $\Gamma_0$ ,  $\bar{\Gamma}_0$  and perturbed orbits  $\Gamma$ ,

$\bar{\Gamma}$  are positioned far away from each other, the generic picture of encounters has no structural changes. One can see only slight changes in their pairwise differences on the fig. 18.

<sup>†</sup> FACULTY OF PHYSICS, UNIVERSITY DUISBURG-ESSEN, LOTHARSTR. 1, 47048 DUISBURG, GERMANY;

*E-mail address:* `boris.gutkin@uni-duisburg-essen.de`, `vladimir.al.osipov@gmail.com`